

Dissertation zur Erlangung des Doktorgrades
der Fakultät für Chemie und Pharmazie
der Ludwig-Maximilians-Universität München

Cyclin-dependent kinase 5 stabilizes the
hypoxia-inducible factor in hepatocellular carcinoma

-

a novel signaling mechanism with potential therapeutic relevance

Julia Herzog

aus

Ehingen, Deutschland

2014



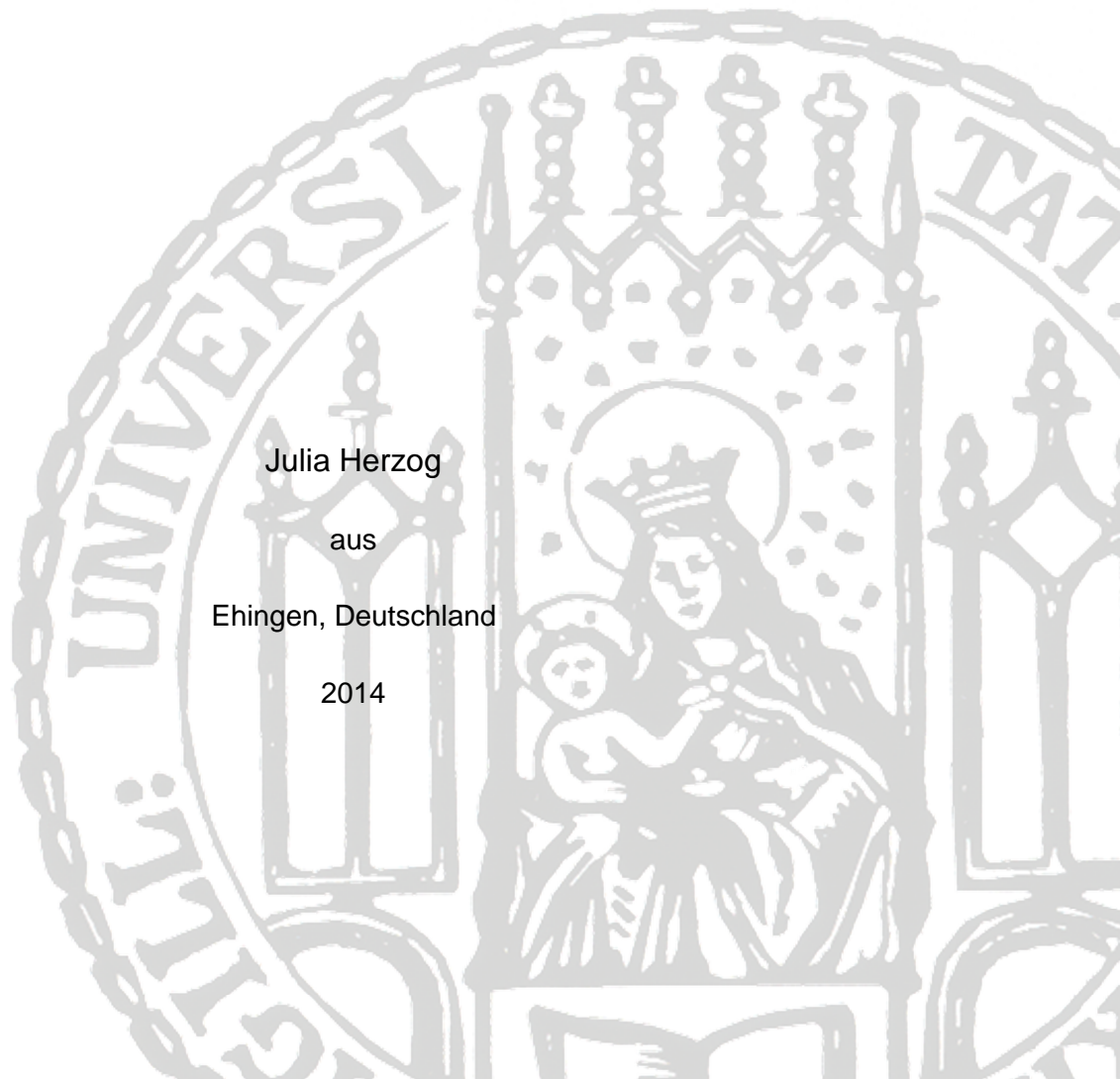
Dissertation zur Erlangung des Doktorgrades
der Fakultät für Chemie und Pharmazie
der Ludwig-Maximilians-Universität München

Cyclin-dependent kinase 5 stabilizes the
hypoxia-inducible factor in hepatocellular carcinoma

-

a novel signaling mechanism with potential therapeutic relevance

Julia Herzog
aus
Ehingen, Deutschland
2014



Erklärung

Diese Dissertation wurde im Sinne von §7 der Promotionsordnung vom 28. November 2011 von Herrn Prof. Dr. Stefan Zahler betreut.

Eidesstattliche Versicherung

Diese Dissertation wurde eigenständig und ohne unerlaubte Hilfe erarbeitet.

München, den 11. Februar 2015

Julia Herzog

Dissertation eingereicht am:	01.12.2014
1. Gutachter:	Herr Prof. Dr. Stefan Zahler
2. Gutachter:	Frau Prof. Dr. Angelika M. Vollmar
Mündliche Prüfung am:	28.01.2015

Meinen Eltern

CONTENTS

1. INTRODUCTION.....	11
1.1 Angiogenesis.....	11
1.1.1 The process of angiogenesis.....	11
1.1.2 Inhibitors of angiogenesis in cancer therapy.....	12
1.2 Hepatocellular carcinoma	13
1.3 Cyclin-dependent kinase 5.....	13
1.3.1 CDK5 in cancer	14
1.3.2 Role of CDK5 during angiogenesis.....	14
1.3.3 CDK5 inhibitors	14
1.4 Hypoxia-inducible factors.....	15
1.4.1 HIF-1 α : structure and function.....	15
1.4.2 HIFs in angiogenesis and cancer	18
1.5 Aim of the study.....	19
2. MATERIALS AND METHODS.....	21
2.1 Materials.....	21
2.1.1 Compounds.....	21
2.1.2 Reagents and technical equipment	21
2.2 Cell Culture.....	23
2.2.1 Solutions and Reagents	23
2.2.2 Endothelial cells	24
2.2.3 Cancer cells	24
2.3 Transfection procedures	25
2.3.1 CDK5 siRNA	25
2.3.2 CDK5 shRNA	25
2.3.3 CDK5 overexpression	25
2.3.4 S687A and S687E HA-HIF-1 α	25
2.3.5 pGL4.27(HIF-REluc2P), pGL4.74(hRluc/TK).....	25

2.4	Immunohistochemistry	26
2.5	Immunocytochemistry	26
2.6	Western blot	27
2.7	Quantitative Real-time PCR	29
2.8	Kinase activity assay	29
2.9	Immunoprecipitation	29
2.10	Co-immunoprecipitation	30
2.11	Mass spectrometry	30
2.12	Site-directed mutagenesis	30
2.13	Dual-Luciferase Assay	31
2.14	Hypoxic chamber assay	31
2.15	<i>In vivo</i> experiments	31
2.16	Statistical analysis	32
3.	RESULTS.....	34
3.1	Pharmacological CDK5 inhibition significantly inhibits angiogenesis <i>in vivo</i>	34
3.2	HIF protein level is regulated by CDK5 in endothelial cells	36
3.3	The transcription of HIF target genes is down-regulated in endothelial cells upon CDK5 inhibition	41
3.4	HIF protein level is regulated by CDK5 in hepatocellular carcinoma cells	42
3.5	The transcription of HIF target genes and transcriptional activation of HIF is down-regulated in HCC cells upon CDK5 inhibition	45
3.6	CDK5 inhibition leads to a reduction of HIF-1 α <i>in vivo</i>	47
3.7	CDK5 directly interacts with HIF-1 α preventing its proteasomal degradation	48
3.8	CDK5 phosphorylates HIF-1 α at serine 687 leading to the stabilization of the transcription factor	49
4.	DISCUSSION.....	53
4.1	Targeting HIFs via CDK5 inhibition in cancer therapy	53
4.2	Anti-angiogenic therapy as treatment strategy for hepatocellular carcinoma.....	53
4.3	Relevance of HIF-1 α and HIF-2 α inhibition in HCC.....	54

4.4	CDK5 phosphorylates HIF – the importance of post-translational modifications in the regulation of HIF stability and activation.....	54
4.5	Involvement of CDK2 in HIF stabilization	55
4.6	CDK5 inhibitors as therapeutic options in HCC therapy	56
4.7	Conclusion and future perspectives	57
5.	SUMMARY.....	59
6.	REFERENCES.....	61
7.	APPENDIX.....	69
7.1	Supplementary data.....	69
7.1.1	Mass spectra.....	69
7.1.2	Sequence analyses of S687A and S687E mutants	71
7.2	Abbreviations.....	77
7.3	Publications	79
7.3.1	Original publication.....	79
7.3.2	Poster presentations	79
7.4	Danksagung	81

LIST OF FIGURES

Figure 1: Multi-step cascade of tumor angiogenesis.....	12
Figure 2: Chemical structure of olomoucine and (R)-roscovitine.....	15
Figure 3: Domains and post-transcriptional modifications of HIF-1 α	16
Figure 4: Oxygen-dependent degradation of HIF-1 α	17
Figure 5: Pharmacological inhibition of CDK5 reduces vascular density in a HUH7 xenograft tumor model.	34
Figure 6: Pharmacological inhibition of CDK5 reduces vascular density in a diethylnitrosamine-induced orthotopic liver tumor model as well as in a HepG2 xenograft tumor model.	35
Figure 7: DFO-induced protein level of HIF-1 α is reduced upon CDK5 inhibition in endothelial cells.....	37
Figure 8: Hypoxic chamber-induced HIF-1 α protein level is reduced upon CDK5 inhibition in endothelial cells.....	38
Figure 9: The protein level of HIF-1 α correlates with CDK5 protein level in endothelial cells also under normoxia.	39
Figure 10: HIF-2 α protein level is reduced by CDK5 inhibition in endothelial cells.	39
Figure 11: CDK2 inhibition also decreases HIF-1 α protein level in endothelial cells.	40
Figure 12: Pharmacological inhibition or knockdown of CDK5 reduces the transcription of HIF target genes in endothelial cells.	41
Figure 13: CDK5 knockdown clones 1 and 4 show a significantly reduced CDK5 protein level in liver tumor cells.....	42
Figure 14: HIF-1 α protein level correlates with CDK5 protein level in liver tumor cells.....	43
Figure 15: The protein level of HIF-1 α correlates with CDK5 protein level in liver tumor cells also under normoxia.	44
Figure 16: HIF-2 α protein level is reduced by CDK5 inhibition in liver tumor cells.....	44
Figure 17: Pharmacological inhibition or distinct knockdown of CDK5 reduces the transcription of HIF target genes in liver tumor cells.	45
Figure 18: Pharmacological inhibition or distinct knockdown of CDK5 reduces the transcriptional activity of HIF-1 α in liver tumor cells.	46
Figure 19: Pharmacological inhibition or distinct knockdown of CDK5 reduces the protein level of HIF-1 α in a HUH7 xenograft tumor model.	47
Figure 20: CDK5 directly interacts with HIF 1 α and protects it from proteasomal degradation.	48
Figure 21: Recombinant P35/CDK5 phosphorylates recombinant HIF-1 α <i>in vitro</i>	49
Figure 22: CDK5 phosphorylates HIF-1 α at serine 687.	50

Figure 23: Phosphorylation of HIF-1 α at serine 687 by CDK5 promotes the stability of the transcription factor.....	51
Figure 24: CDK5 stabilizes HIF, promoting angiogenesis in HCC.....	59
Figure 25: MS/MS spectrum and fragmentation table of peptide ⁶⁸³ SHPRSPNVLSVALSQR ₆₉₈ of HIF-1 α	69
Figure 26: MS/MS spectrum and fragmentation table of peptide ⁶⁸³ SHPRSPNVLSVALSQR ₆₉₈ of HIF-1 α	70
Figure 27: Point mutations at serine 687 to either alanine or glutamate were introduced in HIF-1 α by site-directed mutagenesis.	76

LIST OF TABLES

Table 1: Reagents	21
Table 2: Technical equipment.....	22
Table 3: Primary antibodies	27
Table 4: Secondary antibodies	28
Table 5: Western Blot solutions	28
Table 6: PCR primer and probes	29

INTRODUCTION

1. INTRODUCTION

1.1 Angiogenesis

Angiogenesis, the formation of new blood vessels from preexisting ones (1), is involved in many physiological processes during reproduction, development and wound repair. However, it is also part of many pathophysiological processes, including ischemic, inflammatory, infectious and immune disorders (1, 2). Since the establishment of new blood vessels provides growing tumors with oxygen and nutrients (1), the induction of angiogenesis is regarded as one of the hallmarks of cancer (3).

1.1.1 The process of angiogenesis

Angiogenesis is a multi-step process, which is controlled by stimulators and inhibitors (4). Normally, vasculature is quiescent and only a small portion of endothelial cells is proliferating (5, 6). However, if the amount of pro-angiogenic factors such as vascular endothelial growth factor (VEGF) increases due to stimuli like hypoxia, endothelial cells undergo the “angiogenic switch” (7) and are activated (8) (Fig. 1/1). Tumors as well as activated endothelial cells secrete matrix-metalloproteinases (MMPs). The vascular basement membrane is degraded and endothelial cells migrate in order to form sprouts (Fig. 1/2). Integrins are upregulated facilitating endothelial cells to bind to extracellular membranes. Finally, new capillaries are formed out of proliferating endothelial cells as well as precursor bone-marrow-derived endothelial cells ((2), Fig. 1/3, Fig. 1/4).

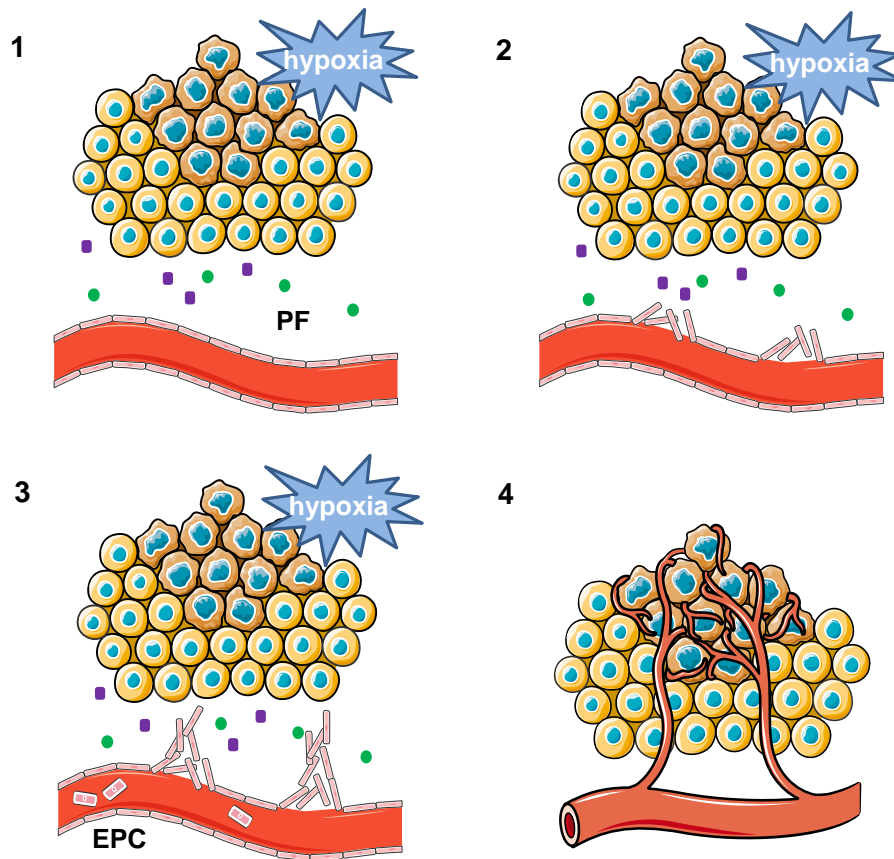


Figure 1: Multi-step cascade of tumor angiogenesis.

Stimuli like hypoxia induce the secretion of pro-angiogenic factors by tumors as well as endothelial cells (1). Thereby endothelial cells get activated, migrate (2) and proliferate to form new sprouts. Precursor bone-marrow-derived endothelial cells also contribute to the vessel formation (3). New sprouts supply the tumor with nutrients and oxygen (4). Abbreviations: PF, pro-angiogenic factors; EPC, endothelial progenitor cells.

1.1.2 Inhibitors of angiogenesis in cancer therapy

Since tumor progression and invasion as well as the formation of metastasis depends on its blood supply, inhibitors of angiogenesis have become of increasing interest in recent years (1). The most notable anti-angiogenic drugs currently used for cancer therapy such as the antibody bevacizumab (Avastin, Genentech/Roche) (1) and the multikinase inhibitors sorafenib (Nexavar, Bayer) and sunitinib (Sutent, Pfizer) target VEGF signaling (9). However, patients inescapably develop resistances including the upregulation of other growth factors and cytokines (10), as well as the induction of hypoxia inducible factors (HIFs) (11). So there is a great need for new therapeutic options which could target such evasive mechanisms, finally leading to a higher efficacy of anti-angiogenic therapy.

1.2 Hepatocellular carcinoma

Hepatocellular carcinoma (HCC) is the third leading cause of cancer related death in the world (12). It is highly prevalent in Asian countries due to widely distributed hepatitis B virus infections (13). However, there is also a growing incidence in Western countries, because of increasing rates of hepatitis C virus infections (14). The majority of HCC patients have an impaired liver function, up to 80% are suffering from cirrhosis (15). This leads to altered pharmacokinetics, making it very difficult to determine the right drug dose for treatment. Although some cytotoxic chemotherapeutics such as doxorubicin or cisplatin have shown antitumor activity in HCC patients, the survival benefit is very limited (9). To date, no satisfying systemic treatment against HCC exists. Even after surgical therapy there is a high rate of tumor recurrence (16).

HCC is one of the most vascularized solid tumors (17) showing an increased *VEGF* expression (18) and a direct correlation of high VEGF levels with worse overall survival in patients (19). Furthermore, angiogenesis in HCC correlates with the risk of vascular invasion and metastasis (20, 21). Therefore, targeting tumor angiogenesis might be a useful tool for HCC treatment (22). First pre-clinical studies with anti-angiogenic agents had been very promising, but could not be confirmed in clinical trials (23). So far, the multikinase inhibitor sorafenib is the only approved systemic anti-angiogenic drug for advanced-stage HCC. However, the median survival of patients is just increased by 2.8 months in comparison to the control group (9). Thus, further targets have to be identified to improve anti-angiogenic therapy.

1.3 Cyclin-dependent kinase 5

Cyclin-dependent kinase 5 (CDK5) is a serine/threonine kinase which has been identified more than 20 years ago in bovine brain extract (24). It is unique among other CDKs because it is no classical mediator of cell-cycle transitions but is implicated in neuronal development, function and disease (25). In neuronal cells, its activity is mainly regulated by the association with the catalytic subunits p35 and p39. Interaction with their truncated forms p25 and p29 results in deregulation, abnormal target phosphorylation as well as mis-localization. This contributes to the pathogenesis of several diseases, like neurodegeneration (25). Furthermore, the activity of CDK5 is regulated by phosphorylation at Tyr15 by the kinases c-Abelson (c-Abl) and Fyn (26, 27). Already a lot of knowledge is gained about CDK5 in neuronal cells. However, in recent years it has become increasingly clear that CDK5 also has

extra-neuronal functions e.g. in epithelial tissues, the immune system, cancer, metabolism and the endothelium (25).

1.3.1 CDK5 in cancer

Several studies indicate an involvement of CDK5 in different types of cancer. Feldmann *et al.* showed that CDK5 is broadly active in pancreatic cancer cells and that its inhibition reduced invasion, migration and anchorage-independent growth *in vitro* as well as orthotopic tumor formation and systemic metastases *in vivo* (28). Furthermore, Demelash *et al.* suggested a correlation between CDK5 activity and cell migration in lung carcinogenesis (29). CDK5 is also described to be involved in medullary thyroid carcinoma progression and tumorigenesis (30). Interestingly, CDK5 is highly expressed in hepatocellular carcinomas and an inhibition of the kinase has been shown to reduce HCC cell proliferation and clonogenic survival. Additionally, *in vivo* efficacy of CDK5 inhibition was demonstrated in HCC xenograft mouse models (Ehrlich *et al.*, Journal of Hepatology, in revision).

1.3.2 Role of CDK5 during angiogenesis

Recent findings demonstrate that CDK5 is also a key regulator of angiogenesis (31). CDK5 inhibition was shown to reduce endothelial cell motility *in vitro* and *in vivo* by decreasing the activity of the small GTPase Ras-related C3 botulinum toxin substrate 1 (Rac1), leading to a disorganized actin cytoskeleton (31). Moreover, a role of CDK5 in endothelial cell growth has been demonstrated, as high levels of CDK5 are found in proliferating bovine aortic endothelial cells and CDK5 is upregulated by basic fibroblast growth factor. Additionally, endothelial cell proliferation has been described to be inhibited by down-regulation of CDK5 (32) and CDK5 activity is shown to correlate with VEGF expression in pituitary adenomas (33).

1.3.3 CDK5 inhibitors

CDK5 has been identified to contribute to several pathological processes. Besides its involvement in neurodegenerative diseases such as Alzheimer's (34-36) and Parkinson's disease (37) as well as cancer, it is also connected to Huntington's disease (38), stroke (39), pain signaling (40, 41) and pancreatic insulin secretion (42). Therefore, the development of inhibitors is of great interest. The earliest well-known inhibitors of CDKs are olomoucine (43) and roscovitine (Seliciclib CYC202) (44), which are 2,6,9-trisubstituted purines (45) (Fig. 2).

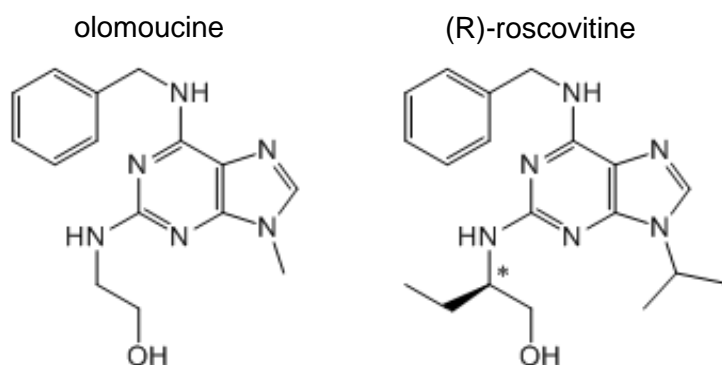


Figure 2: Chemical structure of olomoucine and (R)-roscovitine.

However, they do not inhibit CDK5 specifically, since they generally interact with the ATP-binding site of CDKs (25). Besides CDK5, olomoucine also targets CDK1 and CDK2 (46) and roscovitine additionally inhibits CDK1, CDK2, CDK7 and CDK9 (44). There are non-purine compounds like indirubins, paullones or aloisins (47-49) and also further developed roscovitine derivatives such as BA12 and BP14 (50) which show a greater potency than roscovitine, but without being more selective. Nevertheless, diseases are often multi-factorial and targeting more than one kinase might even be beneficial.

1.4 Hypoxia-inducible factors

Hypoxia-inducible factor-1 (HIF-1) is a heterodimeric transcription factor, which has recently been described to be a target of Cdk5 in mouse neuronal cells (51). It is composed of an oxygen-dependent α -subunit (HIF-1 α or its paralogs HIF-2 α and HIF-3 α) and a constitutively expressed β -subunit (52, 53). Cells and tissues try to persist hypoxic conditions (around 1% O₂) by the stabilization of HIF-1 thus inducing the transcription of target genes involved in angiogenesis, iron metabolism, glucose metabolism, cell proliferation and survival (53).

1.4.1 HIF-1 α : structure and function

HIF-1 α is a protein of 826 amino acids with a half-life of less than five minutes (54, 55). It is expressed ubiquitously and consists of different domains (Fig. 3): a basic-helix-loop-helix (bHLH) and PER-ARNT-SIM (PAS) domain, necessary to bind “HIF-response-elements” on the DNA and for dimerization with its β -subunit (52, 56).

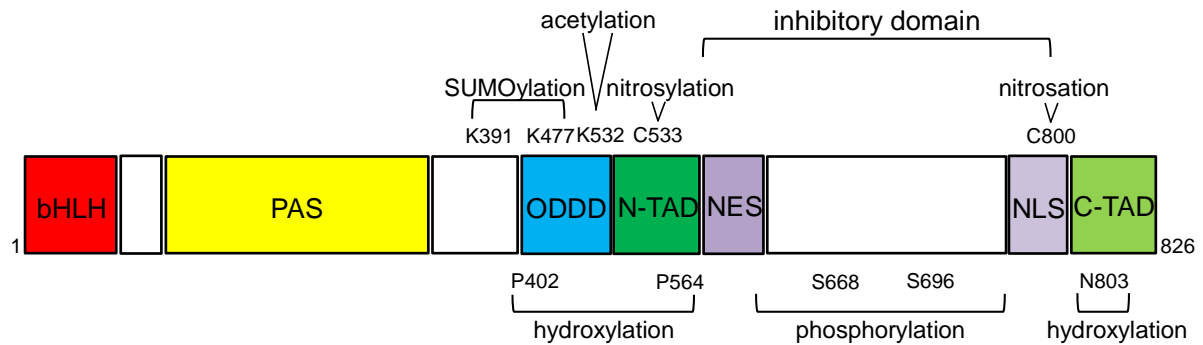


Figure 3: Domains and post-translational modifications of HIF-1 α .

HIF-1 α consists of 826 amino acids, divided into different domains: an N-terminal basic-helix-loop-helix (red) and PER-ARNT-SIM (yellow) domain, important for either DNA binding or dimerization with its β -subunit (52, 56). Furthermore, there is an oxygen-dependent degradation domain (blue), involved in the regulation of HIF-1 α degradation and two transactivation domains called N-TAD (dark green) and C-TAD (light green), important for transcriptional activation. In between those domains lies the inhibitory domain, which negatively regulates transactivation of HIF-1 α . Additionally, a nuclear export signal (dark violet) and a nuclear localization signal (light violet) influence the localization of the transcription factor (52, 57-60). Post-translational modifications such as SUMOylation, hydroxylation, nitrosylation, nitrosation, acetylation and also phosphorylation are located in the C-terminal half and have been shown to be involved in the regulation of HIF-1 α half-life and transcriptional activity (53, 61-63). **Abbreviations:** bHLH, basic-helix-loop-helix; PAS, PER-ARNT-SIM; ODDD, oxygen-dependent degradation domain; N-TAD, N-terminal transactivation domain; NES, nuclear export signal; NLS, nuclear localization signal; C-TAD, C-terminal transactivation domain.

Furthermore, it is composed of an oxygen-dependent degradation domain (ODDD) important for the degradation of the transcription factor by the ubiquitin-proteasome pathway under normoxia (57) as well as two transcriptional activation domains called N-TAD and C-TAD (58, 59, 64). For the regulation of HIF-1 α localization, there are a nuclear localization signal (NLS) and a nuclear export signal (NES) (60). In between the two domains N-TAD and C-TAD lies the “inhibitory domain”. Its deletion has been shown to increase transactivation under normoxia (64). Post-translational modifications of HIF-1 α like SUMOylation, acetylation, nitrosylation, nitrosation, ubiquitination, phosphorylation and also hydroxylation have been shown to influence HIF-1 stability and its transcriptional activity (53, 61-63).

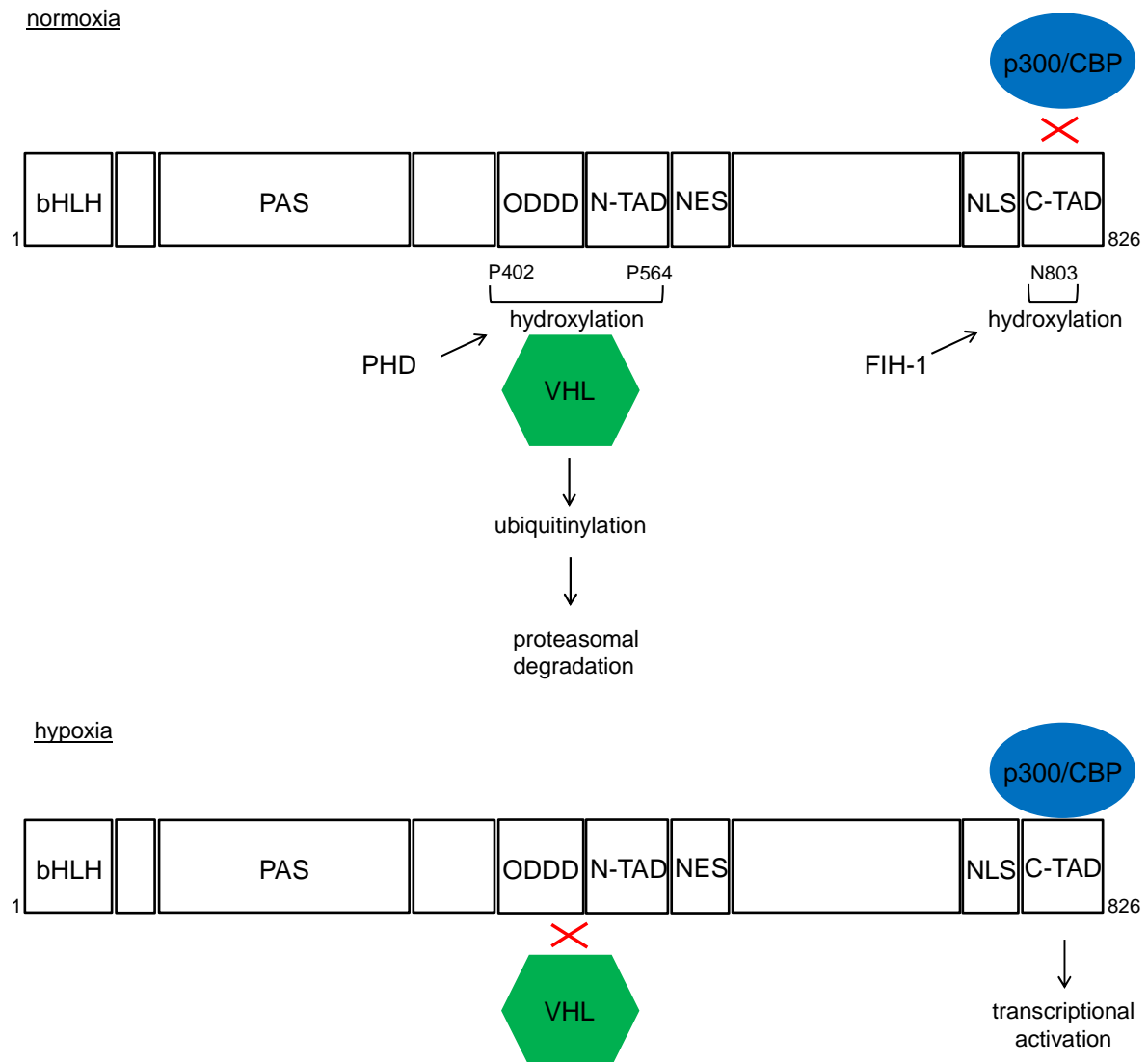


Figure 4: Oxygen-dependent degradation of HIF-1α.

Under normoxic conditions the prolyl-hydroxylase (PHD) hydroxylates HIF-1α at proline 402 and 564, which enables the binding of the von-Hippel-Lindau protein (green). This promotes HIF-1α ubiquitinylation by an E3 ubiquitin-protein ligase finally leading to proteasomal degradation of the transcription factor. Furthermore, hydroxylation of asparagine 803 by factor inhibiting HIF-1 (FIH-1), prevents binding of the transcriptional coactivators p300 and CREB-binding protein (blue) and therefore transcriptional activation. Under hypoxic conditions, HIF-1α is not hydroxylated. VHL cannot bind and HIF-1α is not degraded. Binding of p300 and CBP transcriptionally activates HIF-1α (65). Abbreviations: bHLH, basic-helix-loop-helix; PAS, PER-ARNT-SIM; ODDD, oxygen-dependent degradation domain; N-TAD, N-terminal transactivation domain; NES, nuclear export signal; NLS, nuclear localization signal; C-TAD, C-terminal transactivation domain; VHL, von Hippel-Lindau protein; PHD, prolyl hydroxylase; CBP, cAMP response element-binding protein (CREB) – binding protein; FIH-1, factor-inhibiting-HIF-1.

Under normoxic conditions, HIF-1α is degraded, which is mainly caused by oxygen-dependent hydroxylation at the proline residues 402 and 564 by the prolyl hydroxylase (PHD) (Fig. 4). This enables the binding of the von Hippel-Lindau-protein (VHL), which promotes the ubiquitinylation of HIF-1α by an E3 ubiquitin ligase, targeting HIF-1α for proteasomal degradation. A further hydroxylation at the asparagine residue 803 by the factor-inhibiting-HIF-1 (FIH-1) prevents the binding of the transcriptional coactivators p300 and CREB-binding

protein (CREB). Under hypoxic conditions, HIF-1 α is not hydroxylated, thus not degraded by the VHL pathway but transcriptionally activated by binding of p300/CBP. In consequence, HIF-1 α translocates to the nucleus, dimerizes with its β -subunit and transcription of its target genes is induced (65).

Besides HIF-1 α , its paralog HIF-2 α has also been shown to be a main actor in HIF transcriptional responses. It shares 48% amino acid sequence identity with HIF-1 α and has overlapping functions. However its expression is mainly restricted to the lung, endothelium and carotid body (53, 66-68), but it has also been found in kidney, colonic epithelia, hepatocytes, macrophages, muscle cells and astrocytes (69). The function of HIF-3 α is quite different, since it is suggested to promote or inhibit the activity of other HIF complexes (70-72).

1.4.2 HIFs in angiogenesis and cancer

Hypoxia is a key feature of many tumors. The induction of HIF-1 leads to an altered gene transcription of downstream targets to modulate processes such as glycolysis, proliferation, survival and invasion in order to overcome hypoxic stress (73). Furthermore, the expression of angiogenic factors like vascular-endothelial growth factor (*VEGF*), platelet-derived growth factor (*PDGF*) or placental growth factor (*PLGF*) is induced (74). These factors enhance endothelial or smooth muscle cell proliferation, migration and survival to promote angiogenesis thereby ensuring a sufficient blood supply for the growing tumor (74-76). Several studies have already shown an involvement of HIF-1 in HCC tumorigenesis, progression and metastasis (57). There is compelling evidence, that HCCs overexpress *HIF-1 α* and *HIF-2 α* , which correlates with a poor patient prognosis (77, 78). Since hypoxic tumor areas are much more resistant to chemotherapy and radiation (79) and HIF-1 is involved in many processes promoting tumor growth (80), HIF-1 inhibition is an interesting treatment strategy. There are already inhibitors in clinical assessment, targeting *HIF-1* mRNA transcription, down-regulation of protein synthesis, inhibiting HIF-1 stabilization or subunit heterodimerization, disturbing HIF-1 DNA binding or attenuating transcriptional activity (81, 82). However, those inhibitors still have a very low specificity with undesirable side effects. Therefore, the identification of new targets involved in HIF-1 signaling would putatively help to overcome those limitations.

1.5 Aim of the study

Hepatocellular carcinoma is a rapidly growing tumor reflecting a poor prognosis for patients (83). In many cases the diagnosis is in an already advanced stage, where treatment options are very limited (84). Since it is a highly vascularized tumor, anti-angiogenic therapy has become of increasing interest during the last years (23). First results are very promising, however, evasive mechanisms occur (11).

Thus the aim of this study was to characterize CDK5 as a new potential target for anti-angiogenic therapy of HCC. The involvement of CDK5 in angiogenesis of hepatocellular carcinoma was supposed to be analyzed *in vitro* and *in vivo*. Underlying mechanisms should be identified, focusing on hypoxic signaling, since hypoxia is a key feature of HCC.

MATERIALS AND METHODS

2. MATERIALS AND METHODS

2.1 Materials

2.1.1 Compounds

(R)-roscovitine and deferoxamine were obtained from Sigma-Aldrich, Germany. BA12 (2-[[[2-[(4-aminocyclohexyl)amino]-9-cyclopentyl-purin-6-yl]amino]methyl]-4-chloro-phenol) and BP14 (N2-(4-aminocyclohexyl)-9-cyclopentyl-N6-[[6-(2-furyl)-3-pyridyl]methyl]purine-2,6-diamine) were synthesized (85), dissolved and used (50) as previously described.

2.1.2 Reagents and technical equipment

Table 1: Reagents

Reagent	Producer
Accustain paraformaldehyde	Sigma-Aldrich, Taufkirchen, Germany
AEC substrate	Vector Laboratories, Burlingame, CA, USA
Amphotericin B	AppliChem, Darmstadt, Germany
32P-γ-ATP	Hartmann Analytic, Braunschweig, Germany
Bovine serum albumin (BSA)	Sigma-Aldrich, Taufkirchen, Germany
Bradford Reagent™	Bio-Rad, Munich, Germany
high capacity cDNA Reverse Transcription Kit	Applied Biosystems, San Francisco, CA, USA
Collagenase A	Roche, Mannheim, Germany
Collagen G	Biochrom AG, Berlin, Germany
Complete®	Roche diagnostics, Penzberg, Germany
Dulbecco's Modified Eagles Medium (DMEM)	PAA Laboratories, Pasching, Austria
Dimethylsulfoxide (DMSO)	AppliChem, Darmstadt, Germany
DharmaFECT Transfection reagent	Thermo Scientific, Waltham, MA, USA
EDTA disodium salt dehydrate	Carl Roth, Karlsruhe, Germany
Endothelial Cell Growth Medium (ECGM) with Supplement Mix C-39215	PromoCell, Heidelberg, Germany
Fetal calf serum (FCS)	Biochrom AG, Berlin, Germany
FluorSave™ Reagent mounting medium	Merck, Darmstadt, Germany
Mayer's Hematoxylin Solution	Sigma-Aldrich, Taufkirchen, Germany
Histone H1 (Type III from calf thymus)	Sigma-Aldrich, Taufkirchen, Germany

M199 medium	PAA Laboratories, Pasching, Austria
Non-fat dry milk powder	Carl Roth, Karlsruhe, Germany
Nucleofector™ Kit T	Lonza, Basel, Switzerland
Nucleofector™ Kit HUVEC	Lonza, Basel, Switzerland
Sodium fluoride (NaF)	Merck, Darmstadt, Germany
Sodium orthovanadate (Na ₃ VO ₄)	ICN Biomedicals, Aurora, Ohio, USA
Penicillin	PAA Laboratories, Pasching, Austria
Phenylmethylsulfonylfluoride (PMSF)	Sigma-Aldrich, Munich, Germany
Protein G agarose beads	Sigma-Aldrich, Taufkirchen, Germany
RNeasy Plus Mini Kit	Qiagen, Hilden, Germany
Streptomycin	PAA Laboratories, Pasching, Austria
TaqMan® Gene Expression Master Mix	Applied Biosystems, San Francisco, CA, USA
Targefect-HUVEC	Targeting Systems, El Cajon, CA, USA
Triton X-100	Merck, Darmstadt, Germany
Tween®20	BDH/Prolabo®, Ismaning, Germany
Trypsin	PAN Biotech, Aidenbach, Germany
Vectastain® Universal Elite ABC Kit	Vector Laboratories, Burlingame, CA, USA

Table 2: Technical equipment

Name	Producer
AB7300 RT-PCR	Applied Biosystems, Fosterer City, CA, USA
Nitrocellulose membrane	Hybond-ECL™, Amersham Bioscience, Freiburg, Germany
Nucleofector™II	Amaza, Cologne, Germany
Odyssey 2.1	LI-COR Biosciences, Lincoln, NE, USA
Olympus DP25 camera	Olympus, Hamburg, Germany
Olympus BX41 microscope	Olympus, Hamburg, Germany
SpectraFluor Plus™	Tecan, Crailsheim, Germany
Vi-Cell™ XR	Beckman Coulter, Fullerton, CA, USA
X-ray film (Super RX)	Fuji, Düsseldorf, Germany
LSM 510 META confocal microscope	Zeiss, Jena, Germany

2.2 Cell Culture

2.2.1 Solutions and reagents

PBS (pH 7.4)

NaCl	123.3 mM
Na ₂ HPO ₄	10.4 mM
KH ₂ PO ₄	3.2 mM
H ₂ O	

PBS+Ca²⁺/Mg²⁺ (pH 7.4)

NaCl	136.9 mM
Na ₂ HPO ₄	8.1 mM
KH ₂ PO ₄	1.5 mM
KCl	2.7 mM
MgCl ₂	0.5 mM
CaCl ₂	0.7 mM
H ₂ O	

ECGM

Supplement Mix	4.7%
FCS	10%
Amphotericin B	0.25%
Penicillin	10.000 U/ml
Streptomycin	10%
ECGM	

DMEM

FCS	10%
Penicillin	10.000 U/ml
Streptomycin	10%
DMEM	

Trypsin/EDTA

Trypsin	0.05%
EDTA	0.02%
PBS	

Collagen G

Collagen G	0.001%
PBS	

2.2.2 Endothelial cells

Human umbilical vein endothelial cells (HUVECs) were isolated by digesting umbilical veins with collagenase A (0.1 g/L) for 45 min at 37°C. Prior to digestion, umbilical cords were washed with pre-warmed PBS+Ca²⁺/Mg²⁺. Finally, enzymatic reaction was stopped and cells were washed out the vein with stopping medium (M199 with 10% FCS). Freshly isolated HUVECs were centrifuged (180 g, 5 min, RT), resuspended in endothelial cell growth medium (ECGM) and seeded into a 25 cm² flask. Cells were grown in ECGM supplemented with penicillin (10.000 U/mL) and streptomycin (10%) at 37°C and 5% CO₂ until they were confluent. For passaging they were washed with PBS, detached with trypsin/ethylene diamine tetraacetic acid (EDTA, T/E) and centrifuged (180 g, 5 min, RT) after the addition of stopping medium. Afterwards the pellet was resuspended in ECGM and cells were transferred into a 75 cm² flask. For all experiments, HUVECs were used in passage two and cell culture devices were coated with 0.001% Collagen G for 20 min prior to cell seeding. Human umbilical cords were kindly provided by local hospitals in accordance with the declaration of Helsinki.

2.2.3 Cancer cells

HUH7 cells were obtained from the Japanese Collection of Research Bioresources (JCRB). Cells were grown in Dulbecco's Modified Eagle Medium (DMEM) containing 10% fetal calf serum (FCS) at 37°C and 5% CO₂ until they were confluent. HUH7 cells were passaged 1:5 twice a week. Cells were washed with PBS and detached with EDTA T/E. Finally, cells were seeded in DMEM with 10% FCS. For experiments, cells were used up to passage 30 and cell culture devices were coated with 0.001% Collagen G for 20 min prior to cell seeding.

For long-term storage, confluent cells of a 150 cm² flask were detached, centrifuged (180 g, 5 min, RT) and resuspended in DMEM containing 20% FCS (not heat inactivated) and 10% dimethyl sulfoxide (DMSO). Aliquots in cryovials were stored at -80°C for 24 h and then transferred to liquid nitrogen. For thawing, cells were warmed and pre-warmed DMEM (10% FCS) was added. Afterwards, cells were centrifuged (180 g, 5 min, RT), resuspended in DMEM (10% FCS) and seeded into a 25 cm² flask. Medium was changed the next day and cells were passaged at about 80% confluency as described above.

2.3 Transfection procedures

HUVECs were either transfected with a Targefect/Virofect mixture used for siRNA or a Targefect/Peptide Enhancer mixture used for plasmids or by electroporation using NucleofectorTMII according to the manufacturer's protocol. HUH7 cells were transfected with DharmaFECT Transfection reagent following the manufacturer's instructions.

2.3.1 CDK5 siRNA

CDK5 was silenced with an equal mixture of two different ON-TARGETplus CDK5 siRNAs (J-003239-09 and J-003239-10; Dharmacon, USA). ON-TARGETplus Non-targeting (nt) siRNA (D-001810-01; Dharmacon, USA) served as a control. Silencing efficiency was detected by western blot analysis.

2.3.2 CDK5 shRNA

In HUH7 cells CDK5 silencing by shRNA was performed as previously described (Ehrlich *et al.*, Journal of Hepatology, in revision). CDK5 MISSION® shRNA Lentiviral Transduction Particles (Vector: pLKO.1-puro; SHCLNV-NM_004935; Clone ID: (1) TRCN0000021465, (2) TRCN0000021466, (3) TRCN0000021467, (4) TRCN0000194974, (5) TRCN0000195513; Sigma-Aldrich, Germany) and MISSION® pLKO.1-puro Non-Mammalian shRNA Control Transduction Particles (Sigma-Aldrich SHC002V, Germany) were used according to the manufacturer's protocol.

2.3.3 CDK5 overexpression

HUVECs and HUH7 cells were cotransfected with 3 µg of CDK5-HA (Addgene 1872, van den Heuvel S. (86)) and P35 (Addgene 1347, Tsai Li-Huei), respectively. Transfection of 3 µg of pCMV-Neo-Bam (Addgene, 16440, Vogelstein B. (87)) served as a control. Overexpression efficiency was detected after 24 h by western blot analysis.

2.3.4 S687A and S687E HA-HIF-1α

3 µg of alanine-mutated HIF (S687A) and glutamate-mutated HIF (S687E), generated by site-directed mutagenesis (see 2.12), were transfected into HUH7 cells followed by an incubation time of 24 h. Wildtype HIF-1α (wt, Addgene 18949, Kaelin W. (88)) and an empty pcDNA3 (Invitrogen, Germany) vector served as control (3 µg, 24 h). For Luciferase Assay 0.3 µg of either pcDNA3, wt, S687A or S687E vector were used for transfection.

2.3.5 pGL4.27(HIF-REluc2P), pGL4.74(hRluc/TK)

HUH7 cells were transfected with 3 µg of the firefly luciferase containing vector pGL4.27(HIF-REluc2P) (Promega, USA) and with 0.3 µg of the renilla luciferase containing vector pGL4.74(hRluc/TK) (Promega E692A, USA).

2.4 Immunohistochemistry

Tissue sections from the HUH7 or HepG2 xenograft tumor model as well as from the orthotopic diethylnitrosamine-induced tumor model were stained using the Vectastain® Universal Elite ABC Kit for antibody detection. AEC served as chromogen. In between the different steps, slides were washed with PBS for 10 min at room temperature (RT). For deparaffinization slides were initially incubated for 15 min in xylol, followed by 20 min in 100% and 20 min in 95% ethanol. For HIF-1 α immunostaining, tissue sections were boiled in TRIS-ethylene glycol tetraacetic acid (EGTA) buffer (10mM Tris Base, 1mM EGTA, 0.05% Tween 20, pH 9.0) for 20 min to demask antigens whereas for CD31 staining slides were incubated with proteinase K (20 μ g/ml) for 20 min at 37°C. Endogenous peroxidase was blocked by incubating the slides in 7.5% hydrogen peroxide for 10 min at RT. Sections were incubated with primary antibodies (HIF-1 α , BD Biosciences 610958, 1:100; CD31, BD Biosciences, 553370, 1:100) for 1 h also at RT. Slides were counterstained with haematoxylin for 30 s and washed with water. Sections were embedded with FluorSave™ Reagent mounting medium, covered with glass slips and pictures of the stained sections were taken with an Olympus BX41 microscope and an Olympus DP25 camera.

2.5 Immunocytochemistry

HUVECs were seeded into μ -slides and incubated until they were confluent. In between the different steps cells were washed with PBS+Ca²⁺/Mg²⁺. Cells were fixed with 4% para-formaldehyde for 10 min at RT. Permeabilization of cells was done by treatment with 0.1% Triton X-100 (2 min, RT) followed by a blocking step in 0.2% BSA. Slides were incubated with primary antibodies (CDK5, Invitrogen AHZ0492, 1:100; HIF-1 α , BD Biosciences 610958, 1:100) for 1 h at RT. Afterwards the secondary antibody goat anti-mouse Alexa Fluor 488 (Invitrogen A-11001, 1:400) was applied in combination with Hoechst (Sigma-Aldrich H33342, 5 μ g/ml) and rhodamin-phalloidin (Invitrogen R 415, 1:400) for 30 min at RT. Finally, slides were embedded with FluorSave™ Reagent mounting medium (Merck, Germany), covered with glass slips and pictures of the stained slides were obtained with Zeiss LSM 510 META confocal microscope.

2.6 Western blot

For western blot analysis, cells were washed twice with ice-cold PBS, lysis buffer was added and cells were frozen at -80°C. Afterwards, cells were scraped off on ice and transferred in Eppendorf cups, followed by centrifugation at 18620 g for 10 min at 4°C. Finally, protein amount was determined in supernatants by Bradford analysis and samples were adjusted to the lowest concentration. Proteins were separated by SDS-PAGE and transferred to nitrocellulose membranes by tank blotting. Afterwards, membranes were blocked in 5% non-fat dry milk powder (Blotto) or 5% BSA for 2 h and incubated with primary antibodies overnight at 4°C. Dependent on the detection system the membranes were incubated with different secondary antibodies (2 h, RT): HRP-coupled antibodies were used for chemiluminescence detection by x-ray films whereas IR-fluorescent Reagent conjugated antibodies (Invitrogen, A – 21057, A – 21109; LI-COR IRDye®, 926-32210D, 926-32211D) were used to detect the bands via fluorescence signal at the Odyssey Infrared Imaging system version 2.1.

Table 3: Primary antibodies

Antigen	Catalog No.	Provider	Dilution
Actin	Sc-1615	Santa Cruz	1:1000 in 5% Blotto
β-Tubulin	2146	Cell Signaling	1:1000 in 5% BSA
CDK2	sc-163	Santa Cruz	1:1000 in 5% Blotto
CDK5	AHZ0492	Invitrogen	1:1000 in 5% Blotto
CDK7	2916	Cell Signaling	1:1000 in 5% Blotto
CDK9	sc-13130	Santa Cruz	1:1000 in 5% Blotto
HA	MMS-101R	Covance	1:1000 in 5% Blotto
HIF-1α	610958	BD Biosciences	1:750 in 5% Blotto
HIF-2α	MAB3472	Chemicon	1:1000 in 5% Blotto

Table 4: Secondary antibodies

Antibody	Catalog No.	Provider	Dilution
Goat anti-mouse IgG1: HRP	BZL07046	Biozol	1:1000 in 1% Blotto
Goat anti-rabbit: HRP (H+L)	111-035-144	Dianova	1:1000 in 1% Blotto
Alexa Fluor® 680 Goat anti-mouse IgG (H + L)	A – 21057	Invitrogen	1:10.000 in 1% Blotto
IRDye™ 800CW Goat anti-rabbit IgG (H + L)	926-32211D	LI-COR	1:10.000 in 1% Blotto

Table 5: Western blot solutions

Solutions	Composition
Lysis buffer	Tris/HCl 50 mM, NaCl 150 mM, Nonidet NP-40 1%, sodium deoxycholate 0.25%, SDS 0.1%, activated Na ₂ VO ₄ 300 µM, NaF 1 mM, β-glycerophosphate 3 mM, pyrophosphate 10 mM, Complete® EDTA free 4 mM, PMSF 1 mM, H ₂ O ₂ 600 µM in H ₂ O
5 x SDS sample buffer	Tris/HCl (pH 6.8) 3.125 M, glycerol 50%, SDS 5%, DTT 2%, Pyronin Y 0.025% in H ₂ O
Separation gel 10%/12%	Rotiphorese™ Gel 30 33%/40%, Tris (pH 8.8) 375 mM, SDS 0.1%, TEMED 0.1%, APS 0.05% in H ₂ O
Stacking gel	Rotiphorese™ Gel 30 17%, Tris (pH 6.8) 125 mM, SDS 0.1%, TEMED 0.2%, APS 0.1% in H ₂ O
Electrophoresis buffer	Tris 4.9 mM, glycine 38 mM, SDS 0.1% in H ₂ O
Tank buffer	Tris base 48 mM, glycine 39 mM, methanol 20% in H ₂ O

2.7 Quantitative Real-time PCR

Initially, RNA was isolated by RNeasy Kit according to the manufacturer's protocol. Concentrations and purity of samples were determined with NanoDrop spectrophotometer. RNA was transcribed to cDNA with the high capacity cDNA Reverse Transcription Kit. Real-time PCR was performed with 7300 Real Time PCR system. PCR components were supplied as master mix (TaqMan® Gene Expression Master Mix). For detecting the gene expression a set containing primer and probe for the specific gene was added (Applied Biosystems, USA). *GAPDH* served as housekeeping gene (Biomers, Germany). Calculation of the relative mRNA levels was done as described previously (89).

Table 6: PCR primer and probes

Primer/probe	Catalog No.	Provider	Concentration
<i>EphrinA1</i>	Hs00358886	Applied Biosystems	1 x
<i>VEGFA</i>	Hs00900055	Applied Biosystems	1 x
<i>VEGFR1</i>	Hs01052961	Applied Biosystems	1 x

2.8 Kinase activity assay

Either immunoprecipitated CDK5 or recombinant CDK5/P35 (20 ng, Millipore 14-477, USA) was diluted in 50 µl kinase buffer (50 mM HEPES pH 7.0, 10 mM MgCl₂, 1 mM DTT, 1 mM NaF, 1 mM Na₃VO₄, 1 mM PMSF, 3 mM β-glycerophosphate, 4 mM Complete® EDTAfree). As substrates Histone H1 (2.5 µg, Sigma-Aldrich H5505, USA) or HIF-1α (2.5 µg, Abcam ab48734, UK) were added. Finally 2 µM ATP and 10 µCi 32P-γ-ATP (Hartmann Analytic SRP-301, Braunschweig, Germany) completed the reaction mix. The samples were incubated at 30°C for 20 minutes. Then samples were prepared for SDS-Page gel electrophoresis by adding 5 x SDS Sample buffer and incubating them for 5 minutes at 95°C. Electrophoresis was run for 21 minutes at 100 V followed by another 35 minutes at 200 V. Phosphorylation of substrates was detected via autoradiography. An X-ray film was placed on the gel for 6 up to 48 h at -80°C.

2.9 Immunoprecipitation

Cells were lysed with a buffer containing 50 mM Tris/HCl pH 7.5, 250 mM NaCl, 1 mM EDTA pH 8.0, 10 mM NaF, 1x SIGMAFAST™ Protease Inhibitor. After scraping the cells off, they were incubated for about 30 min on ice. Samples were centrifuged (10.000 g, 10 min, 4°C)

and protein concentrations were adapted. 2 µg antibody (Cdk5; sc-173, Santa Cruz Biotechnology) were added per 500 µg protein followed by an incubation overnight at 4°C. Afterwards each sample was incubated with 25 µL packed Protein G Agarose beads (Sigma-Aldrich, Germany) for 3 h at 4°C. Finally further centrifugation steps followed (14.000 g, 45 s, 4°C) in order to wash the beads.

2.10 Co-immunoprecipitation

Co-immunoprecipitation experiments were performed using the Pierce Crosslink Magnetic IP/Co-IP Kit (Thermo Scientific 88805, USA) according to the manufacturer's protocol. 5 µg of CDK5 antibody (Invitrogen AHZ0492, USA) or HIF-1α antibody (BD Biosciences 610958, Germany) were used for immunoprecipitation. Mouse IgG1 (Abcam ab18443, UK) served as control antibody.

2.11 Mass spectrometry

In mass spectrometry experiments, phosphorylations on either recombinant HIF-1α (2.5 µg, Abcam ab48734, UK), incubated with 20 ng recombinant CDK5/P35 (Millipore, 14-477, USA) and 2 µM ATP at 30°C for 20 min or on HIF-1α immunoprecipitated in deferoxamine treated (6 h) HUH7 cells were analyzed. SDS-Page gel electrophoresis of the different samples was done followed by Coomassie staining. Gels were finally used for mass spectrometry analysis which was performed by Dr. T. Fröhlich from the Laboratory for Functional Genome Analysis (LAFUGA), Gene Center, University of Munich.

2.12 Site-directed mutagenesis

Point mutation in HIF-1α (Addgene 18949, Kaelin W. (88)) at serine 687 was generated by site-directed mutagenesis with primers that contain specific mismatches: 5'GAACAGACAGAAAAATCTCATCCAAGAGCTCCTAACGTGTTATCTGTGCTTTG and 3'CAAAGCGACAGATAACACGTTAGGAGCTCTTGGATGAGATTTTCTGTCTGTTC primers were used for an alanine mutation (S687A) whereas 5'GAACAGACAGAAAAATCTCATCCAAGAGAGCCTAACGTGTTATCTGTGCTTTG and 3'CAAAGCGACAGATAACACGTTAGGCTCTCTTGGATGAGATTTTCTGTCTGTTC were used for a glutamate mutation (S687E). The mutated codons are underlined. Template DNA of mutagenesis PCR was digested with DpnI (New England Biolabs R0176S, Germany). The

PCR-generated mutants were transformed into competent *E.coli* and grown on selective agar (Ampicillin). Mini-prep of selected clones was performed according to the manufacturer's instructions (Qiagen 27106, Germany). The nucleotide sequences of isolated plasmids were verified by sequence analysis performed by MWG Eurofins (Germany) followed by maxi-prep of the correctly mutated clones (Qiagen 12362, Germany) according to the manufacturer's protocol.

2.13 Dual-Luciferase assay

HUH7 cells were seeded into a 96-well plate and transfected with *pGL4.27(HIF-REluc2P)* and *pGL4.74(hRluc/TK)* (Promega, USA). The activity of firefly and renilla luciferases was determined using the Dual-Luciferase Reporter Assay System (Promega E1910, USA) according to the manufacturer's instructions. For measurement, lysed cells were transferred into a white 96-well plate. Luminescence was detected with Orion II Microplate Luminometer (Berthold Detection Systems).

2.14 Hypoxic chamber assay

Cells were cultivated in a hypoxic chamber (Don Whitley Scientific, Whitley H35 Hypoxystation, UK) at 1% O₂ in carbonate-free medium (Biochrom AG L-15 Leibovitz Medium, Germany) supplemented with 10% FCS and penicillin (10.000 U/mL) as well as streptomycin (10%). Control cells were cultivated at around 21% oxygen in a CO₂ free incubator. After 24 h cells were lysed and western blot analysis was performed.

2.15 *In vivo* experiments

All experiments were performed according to Austrian guidelines or German legislation for the protection of animals and approved by the local government authorities. Experiments were carried out as described previously (Ehrlich *et al.*, Journal of Hepatology, in revision, (50)).

HUH7 xenograft tumor model: 3.3*10⁶ of either HUH7 cells or CDK5 knockdown HUH7 cells were subcutaneously injected in 100 µL PBS into the flank of female SCID mice (8–10 weeks). The tumor progression was regularly controlled. Roscovitine treated mice were injected intraperitoneally (150 mg/kg, 100 µL; solvent: PBS/DMSO/Solutol 17:1:2). Seven days after tumor implantation application of roscovitine started and daily injections were

carried on for seven days. Control mice received solvent only. This *in vivo* experiment was performed by Dr. J. Liebl and B. Hager.

HepG2 xenograft tumor model: 5.0×10^6 HepG2 cells were subcutaneously injected into SCID mice (Harlan Laboratories, San Pietro, Italy). Mice were injected intraperitoneally with either 5 mg/kg BA12 or 1 mg/kg BP14 in 100 μ l of 0.01% DMSO every day (17 days). Control mice received DMSO only. This *in vivo* experiment was performed by the group of Prof. Mikulits at the University of Vienna.

Diethylnitrosamine-induced orthotopic tumor model: For tumor development 14-day-old male C57BL/6J mice were intraperitoneally injected with a single dose of diethylnitrosamine (DEN, 25 mg/kg). After eight month of tumor growth, mice were treated with compounds in three cycles for 10 days with a release of the compounds in between the cycles for seven days. Mice were injected intraperitoneally with either 5 mg/kg BA12 or 1 mg/kg BP14 in 100 μ L of 0.01% DMSO. Control mice received DMSO only. This *in vivo* experiment was performed by the group of Prof. Mikulits at the University of Vienna.

2.16 Statistical analysis

Data are expressed as means \pm standard error of mean (SEM) or as Whisker plots with lines indicating maximum and minimum values. The statistical significances were determined using GraphPad Prism 5. Statistical significance is assumed if $p \leq 0.05$. Statistical tests are indicated in the corresponding figure legends.

RESULTS

3. RESULTS

3.1 Pharmacological CDK5 inhibition significantly inhibits angiogenesis *in vivo*

Recent studies reported that CDK5 plays a crucial role during angiogenesis (31). Since CDK5 is highly expressed in hepatocellular carcinoma (Ehrlich *et al.*, Journal of Hepatology, in revision) and HCC is one of the most vascularized solid tumors (17), the effect of CDK5 inhibition on vascularization was investigated in different liver tumor models. CD31 staining of HUH7 tumors from mice treated with roscovitine (rosco), a well-established CDK5 inhibitor (44), revealed a reduced microvascular density as compared to solvent controls. This result was also confirmed by CD34 staining, another well-known endothelial cell marker, which is additionally expressed on hematopoietic stem cells (90) (Fig. 5). The *in vivo* experiments were performed by Dr. J. Liebl and B. Hager.

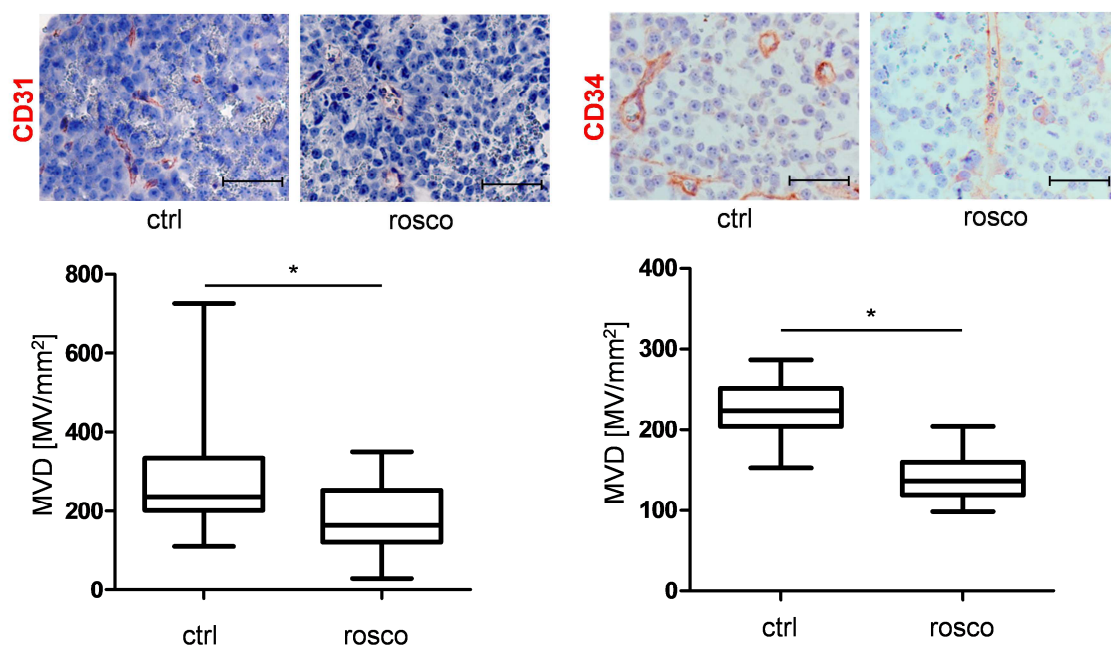


Figure 5: Pharmacological inhibition of CDK5 reduces vascular density in a HUH7 xenograft tumor model.

Immunostaining for CD31 (red) or CD34 (red) and haematoxylin (blue, nuclei) of HCC tumors grown in SCID mice either treated with solvent or roscovitine is shown. The microvessel density (MVD) per square mm was determined. Scale bars: 50 μ m. Non-parametric t-test on Mann-Whitney, * $p < 0.05$, $n = 8$. Whisker lines indicate maximum and minimum values. Immunostaining was performed by Dr. S. Ehrlich.

Furthermore, the effect of the two roscovitine derivatives BA12 and BP14 on vascular density was investigated in a diethylnitrosamine (DEN)-induced orthotopic mouse tumor model (Fig. 6A) as well as in a HepG2 xenograft mouse tumor model (Fig. 6B).

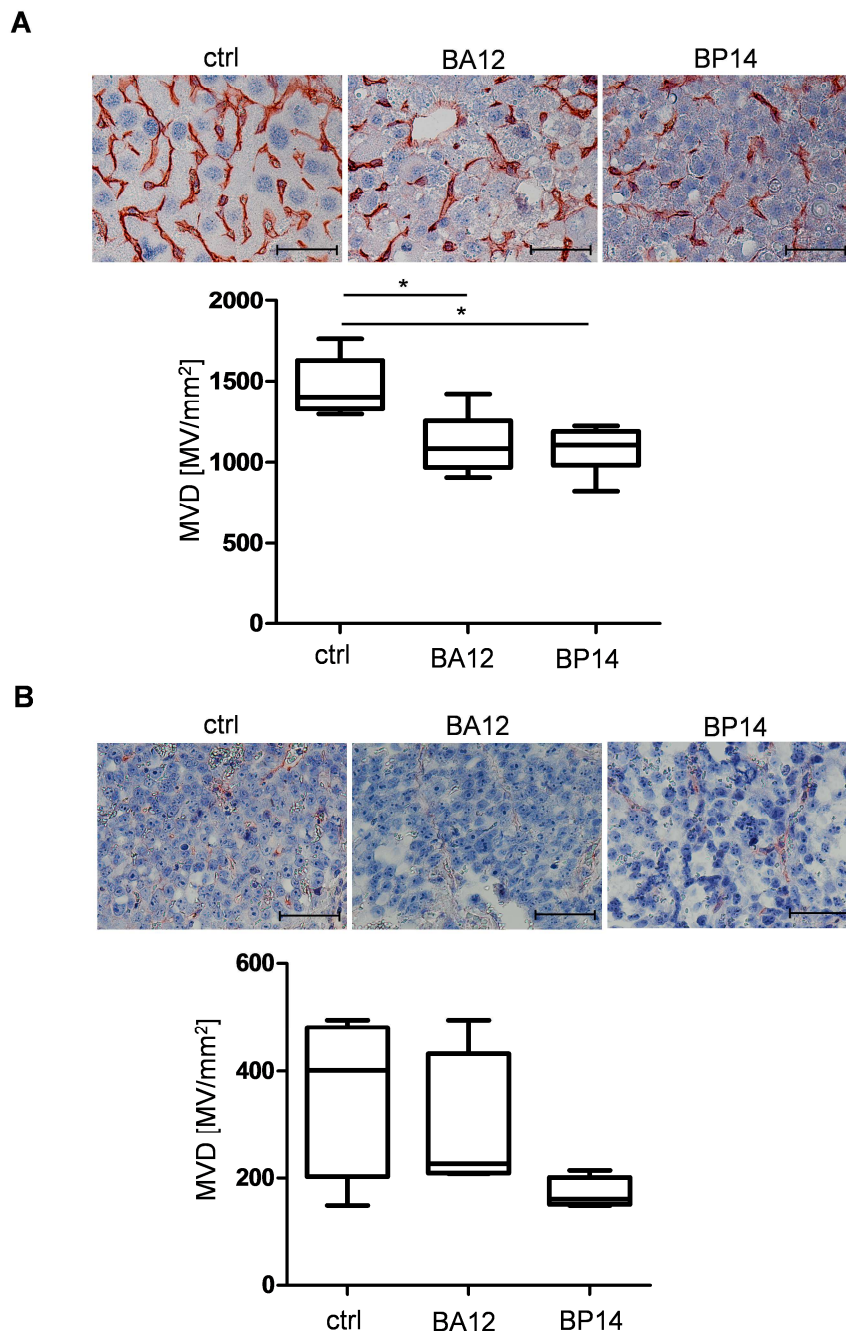


Figure 6: Pharmacological inhibition of CDK5 reduces vascular density in a diethylnitrosamine-induced orthotopic liver tumor model as well as in a HepG2 xenograft tumor model.

(A) Immunostaining for CD31 (red) and haematoxylin (blue, nuclei) of DEN-induced tumors grown in mice either treated with solvents or the roscovitine derivatives BA12 and BP14. The microvessel density per square mm was determined. Scale bars: 50 μ m. Non-parametric t-test on Mann-Whitney, * $p < 0.05$, $n = 5$. Whisker lines indicate maximum and minimum values. **(B)** Immunostaining for CD31 (red) and haematoxylin (blue, nuclei) of HepG2 tumors grown in SCID mice either treated with solvents or the roscovitine derivatives BA12 and BP14. The microvessel density per square mm was determined. Scale bars: 50 μ m. $n = 4$. Whisker lines indicate maximum and minimum values.

Tumors were kindly provided by the group of Prof. Wolfgang Mikulits from the Department of Medicine I of the Medical University of Vienna. The microvessel density was analysed by CD31 immunostaining. The vascular density in tumors of mice treated with BA12 and BP14 was reduced as compared to solvent controls (Fig. 6) in both models.

3.2 HIF protein level is regulated by CDK5 in endothelial cells

In further studies the signaling mechanism putatively responsible for the effects on angiogenesis was investigated. Hypoxia is often a key feature of tumor progression, promoting the expression of angiogenic factors by hypoxia inducible factors (91). Therefore, the effect of either CDK5 inhibition or overexpression on HIF-1 α was examined. Hypoxia was simulated by the iron chelator deferoxamine (DFO) or in a hypoxic chamber (1% O₂). Both, pharmacological inhibition of CDK5 by roscovitine and siRNA mediated down-regulation, decreased the DFO-induced protein level of HIF-1 α in human umbilical vein endothelial cells (HUVECs) (Fig. 7).

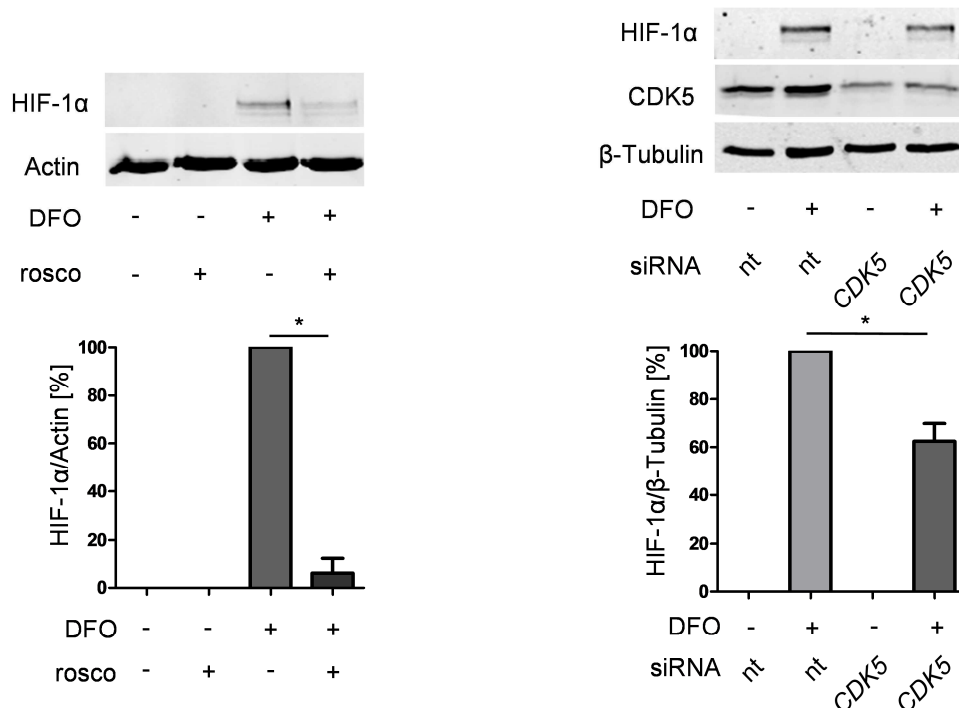
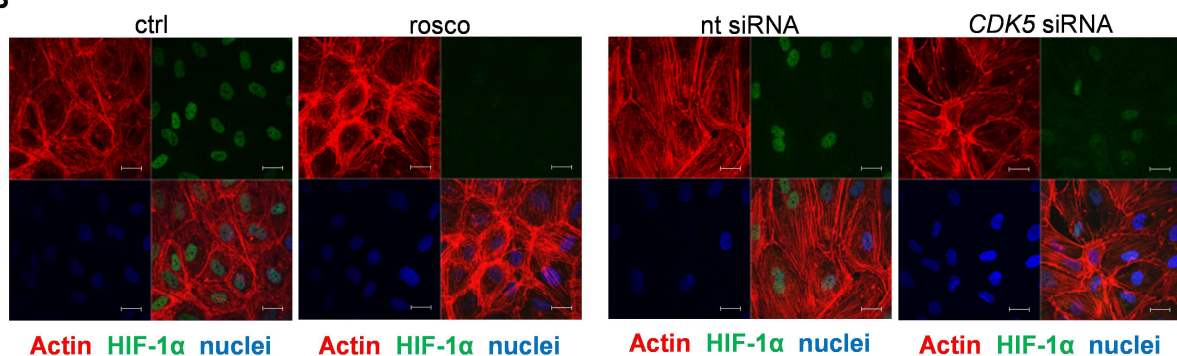
A**B**

Figure 7: DFO-induced protein level of HIF-1α is reduced upon CDK5 inhibition in endothelial cells.

(A) Immunoblots of lysates from HUVECs. CDK5 was either inhibited pharmacologically by roscovitine pretreatment for 30 minutes (30 μM) or transiently down-regulated by siRNA. Lysates were probed with antibodies for HIF-1α, CDK5, Actin or β-Tubulin. To simulate hypoxia HUVECs were treated with 100 μM of the iron chelator deferoxamine for six hours. The quantifications of the corresponding immunoblots are shown. One Way ANOVA on Newman-Keuls, * $p < 0.05$, $n = 3$. Error bars represent mean \pm SEM. **(B)** Immunostaining of HUVECs for HIF-1α, Actin and nuclei. Cells were either untreated or treated with roscovitine or transfected with nt siRNA or CDK5 siRNA. Scale bars: 20 μm.

This was also confirmed for HUVECs cultivated at 1% O₂ in a hypoxic chamber (Fig. 8). In line with these findings, overexpression of P35/CDK5, led to a significantly increased HIF-1 α protein level under normoxic conditions (Fig. 9).

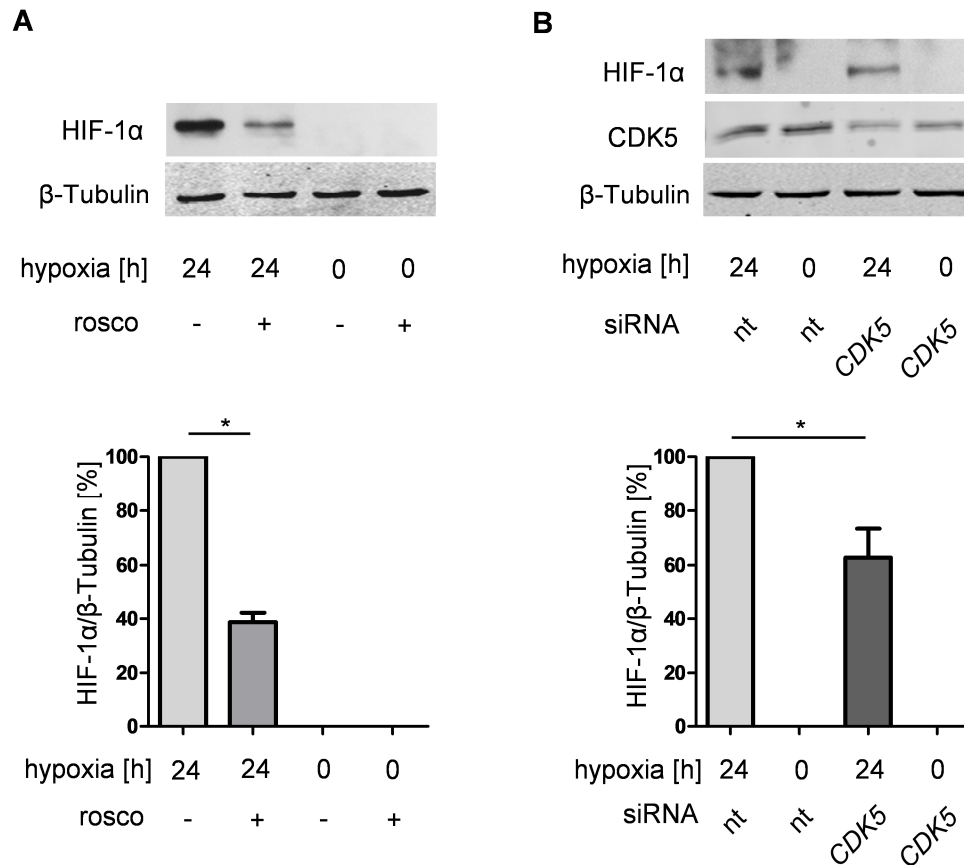


Figure 8: Hypoxic chamber-induced HIF-1 α protein level is reduced upon CDK5 inhibition in endothelial cells.

Immunoblots of lysates from HUVECs either incubated at 21% or 1% oxygen for 24 hours. **(A)** CDK5 was pharmacologically inhibited by roscovitine. Lysates were probed with antibodies for HIF-1 α , CDK5 and β -Tubulin. Below the quantifications of the corresponding immunoblots are shown. One Way ANOVA on Newman-Keuls, * $p < 0.05$, $n = 3$. Error bars represent mean \pm SEM. **(B)** CDK5 was silenced with *CDK5* siRNA. Lysates were probed with antibodies for HIF-1 α , CDK5 and β -Tubulin. Below the quantifications of the corresponding immunoblots are shown. One Way ANOVA on Newman-Keuls, * $p < 0.05$, $n = 3$. Error bars represent mean \pm SEM.

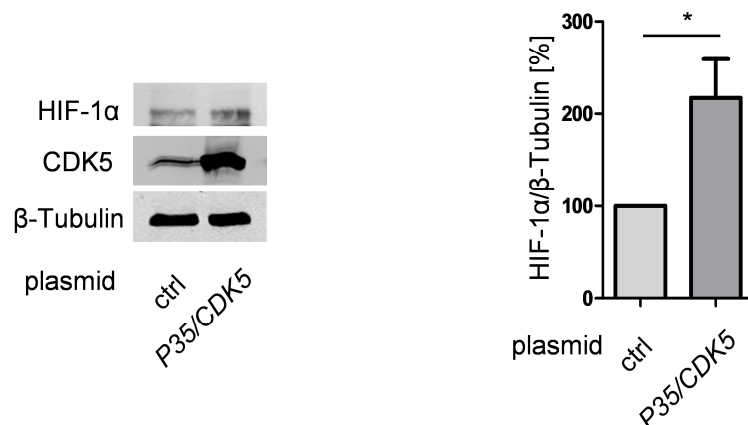


Figure 9: The protein level of HIF-1α correlates with CDK5 protein level in endothelial cells also under normoxia.

Immunoblot shows protein level of HIF-1α in HUVECs either transfected with a control plasmid or with a *P35/CDK5* vector, cultivated under normoxic conditions (21% oxygen). Quantification is shown. One Way ANOVA on Newman-Keuls, * $p < 0.05$, $n = 3$. Error bars represent mean \pm SEM.

Since not only overexpression of HIF-1α but also of HIF-2α is a common feature in hepatocellular carcinoma (83), the effect of CDK5 inhibition on the subunit HIF-2α was additionally analysed. Indeed, roscovitine treatment of HUVECs also led to a decrease of the DFO-induced protein level of HIF-2α (Fig. 10).

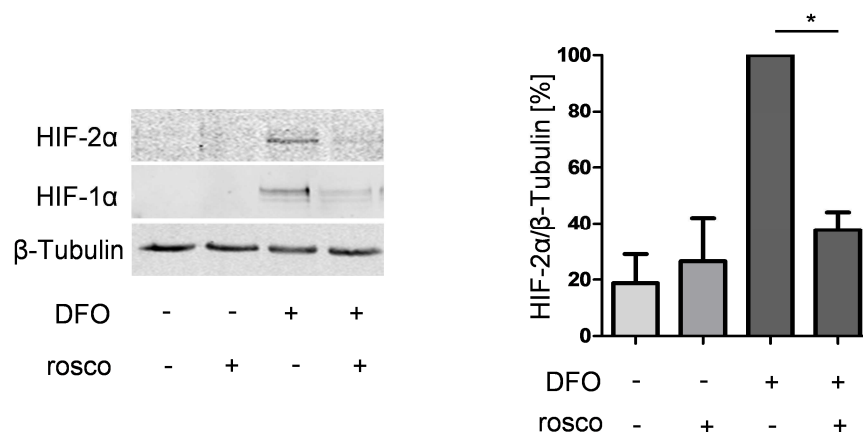


Figure 10: HIF-2α protein level is reduced by CDK5 inhibition in endothelial cells.

Immunoblot for HIF-2α, HIF-1α and β-Tubulin of HUVECs treated with 30 μM roscovitine. Graph displays the quantification. One Way ANOVA on Newman-Keuls, * $p < 0.05$, $n = 3$. Error bars represent mean \pm SEM.

In further experiments the influence of other CDKs on the protein level of HIF-1 α was assessed. Whereas siRNA mediated down-regulation of CDK2 also led to a significant decrease of the DFO-induced protein level of HIF-1 α , CDK7 and CDK9 seemed to have no strong influence on the protein amount of the transcription factor (Fig. 11).

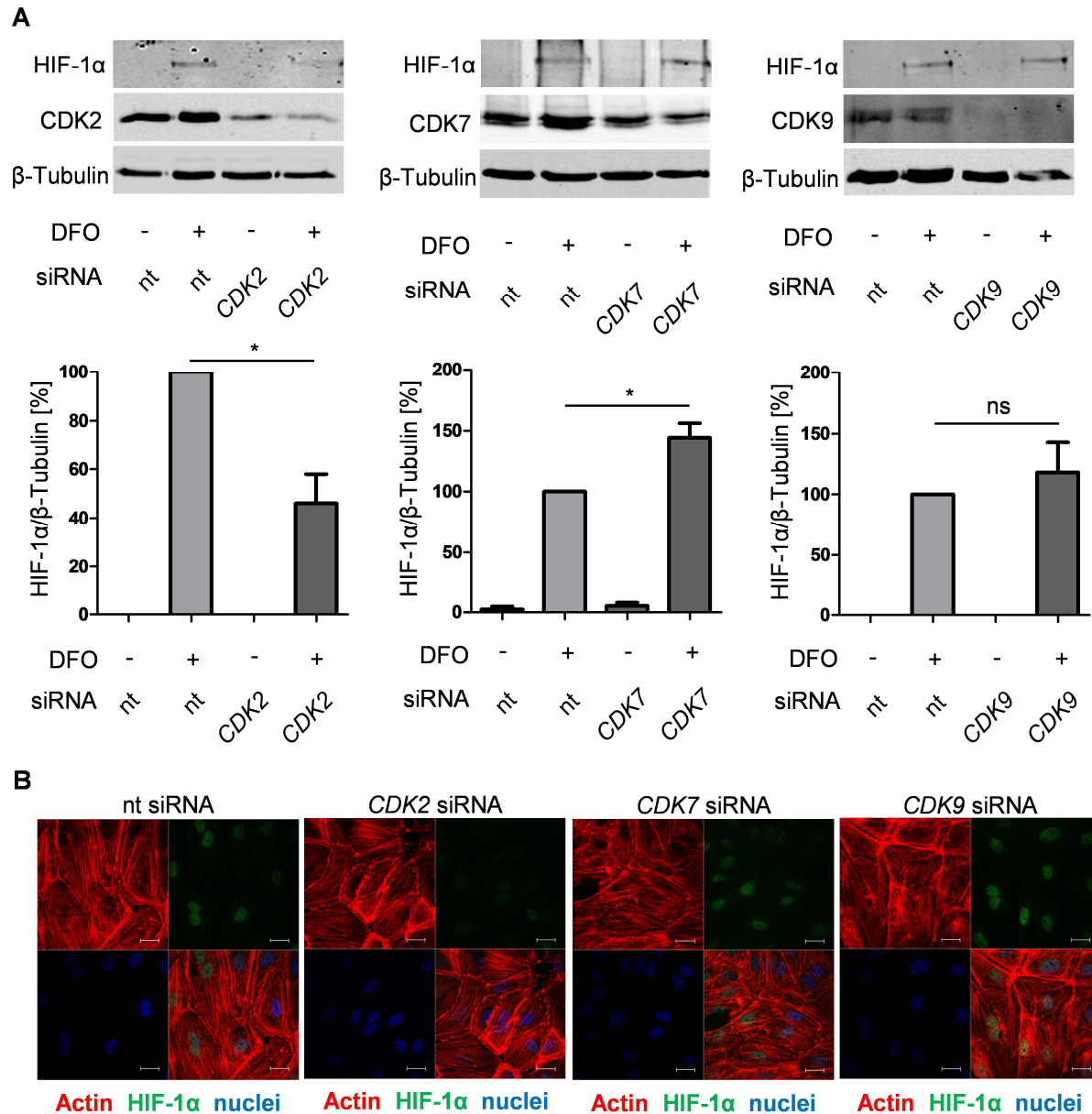


Figure 11: CDK2 inhibition also decreases HIF-1 α protein level in endothelial cells.

(A) Immunoblots of lysates from HUVECs either transfected with *CDK2*, *CDK7* or *CDK9* siRNA. Lysates were probed with antibodies for HIF-1 α , β -Tubulin and the corresponding kinase to check the knockdown. To simulate hypoxia, cells were stimulated with 100 μ M deferoxamine for six hours. The quantifications of the corresponding immunoblots are shown. One Way ANOVA on Newman-Keuls, * $p < 0.05$, $n = 3$. Error bars represent mean \pm SEM. **(B)** Immunostaining of HUVECs for HIF-1 α , Actin and nuclei. Cells were either transfected with non-target siRNA or with *CDK2*, *CDK7* or *CDK9* siRNA. Scale bars: 20 μ m.

3.3 The transcription of HIF target genes is down-regulated in endothelial cells upon CDK5 inhibition

To clarify whether CDK5 also influences the transcriptional activity of HIF, quantitative real-time PCR analysis of HIF target genes *VEGFA* and *VEGFR1* was performed in HUVECs. Both genes are known to be involved in the regulation of angiogenesis (2). The hypoxia-induced increase of the *VEGFA* and *VEGFR1* mRNA levels was significantly decreased after pharmacological CDK5 inhibition (Fig. 12A), as well as upon siRNA mediated down-regulation (Fig. 12B) of CDK5.

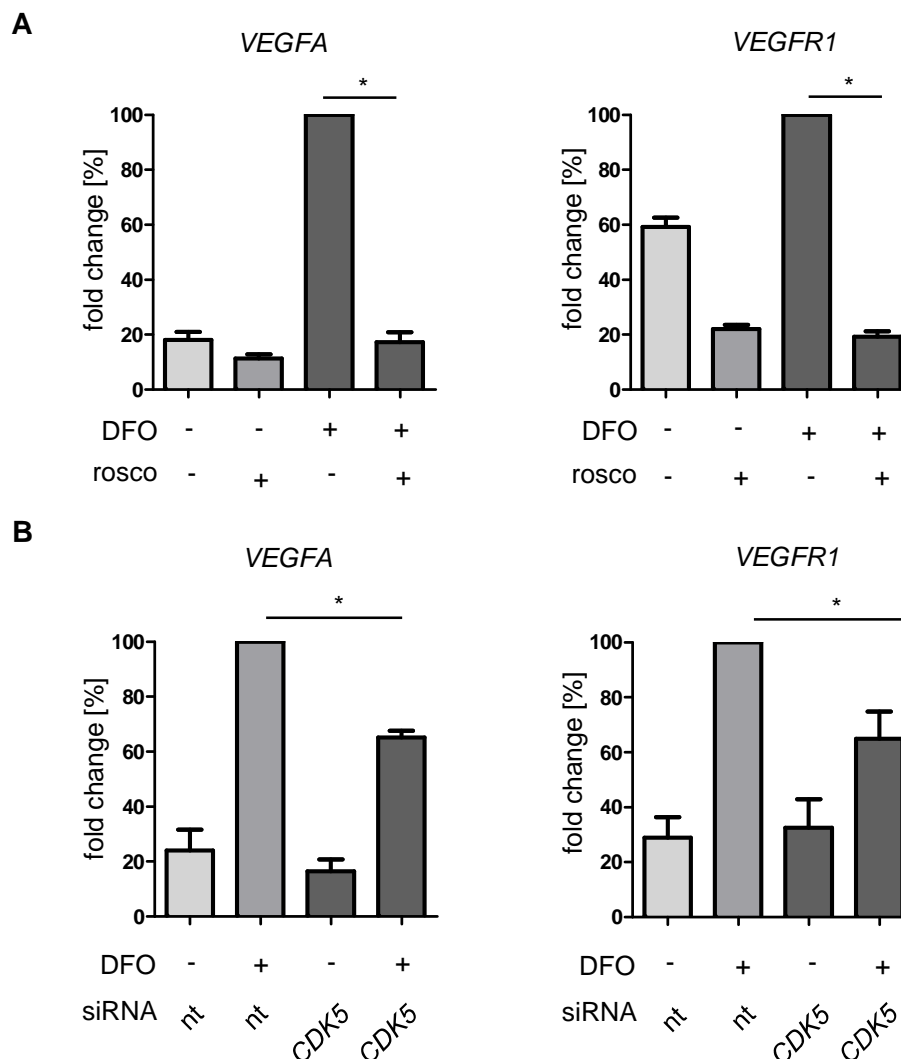


Figure 12: Pharmacological inhibition or knockdown of CDK5 reduces the transcription of HIF target genes in endothelial cells.

(A) Real-time PCR analysis of the HIF target genes *VEGFA* and *VEGFR1* is shown. HUVECs were either untreated or treated with roscovitine. Hypoxia was simulated by treating the cells with 100 μ M deferoxamine for six hours. Graphs display the fold change in percent. One Way ANOVA on Newman-Keuls, * $p < 0.05$, $n = 3$. Error bars represent mean \pm SEM. **(B)** Real-time PCR of *VEGFA* and *VEGFR1* for HUVECs either transfected with nt siRNA or *CDK5* siRNA, treated with 100 μ M deferoxamine for six hours. Graphs display the fold change in percent. One Way ANOVA on Newman-Keuls, * $p < 0.05$, $n = 3$. Error bars represent mean \pm SEM.

3.4 HIF protein level is regulated by CDK5 in hepatocellular carcinoma cells

In order to investigate the effect of CDK5 inhibition on HIF in hepatocellular carcinoma cells (HUH7), CDK5 was either inhibited by roscovitine or stably down-regulated by shRNA. The knockdown level of two independent HUH7 clones (CDK5-1: CDK5 knockdown clone 1, CDK5-4: CDK5 knockdown clone 4) is shown in Fig. 13.

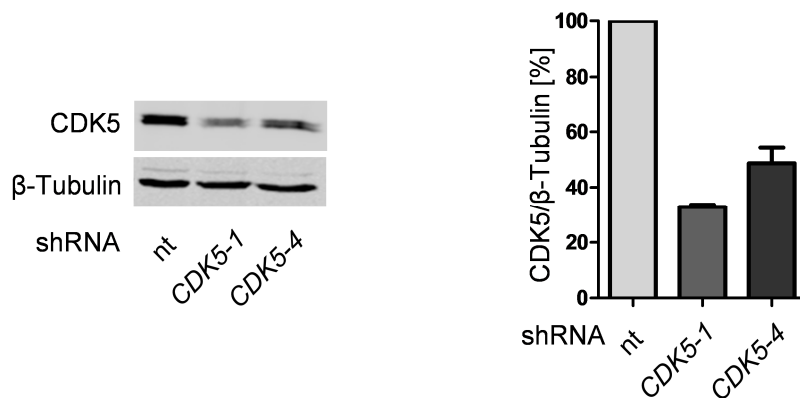


Figure 13: CDK5 knockdown clones 1 and 4 show a significantly reduced CDK5 protein level in liver tumor cells.

Immunoblot for CDK5 and β -Tubulin of lysates from HUH7 cells transfected with *CDK5* shRNA (CDK5-1: clone 1, CDK5-4: clone 4). Graph displays quantification of the knockdown level.

In parallel to the results in HUVECs, CDK5 inhibition either by roscovitine or by stable shRNA mediated down-regulation led to a reduction of the protein level of HIF-1 α in DFO treated HUH7 cells. This result could be confirmed comparing the two independent HUH7 clones, CDK5-1 and CDK5-4, cultivated in a hypoxic chamber at 1% O₂ (Fig. 14).

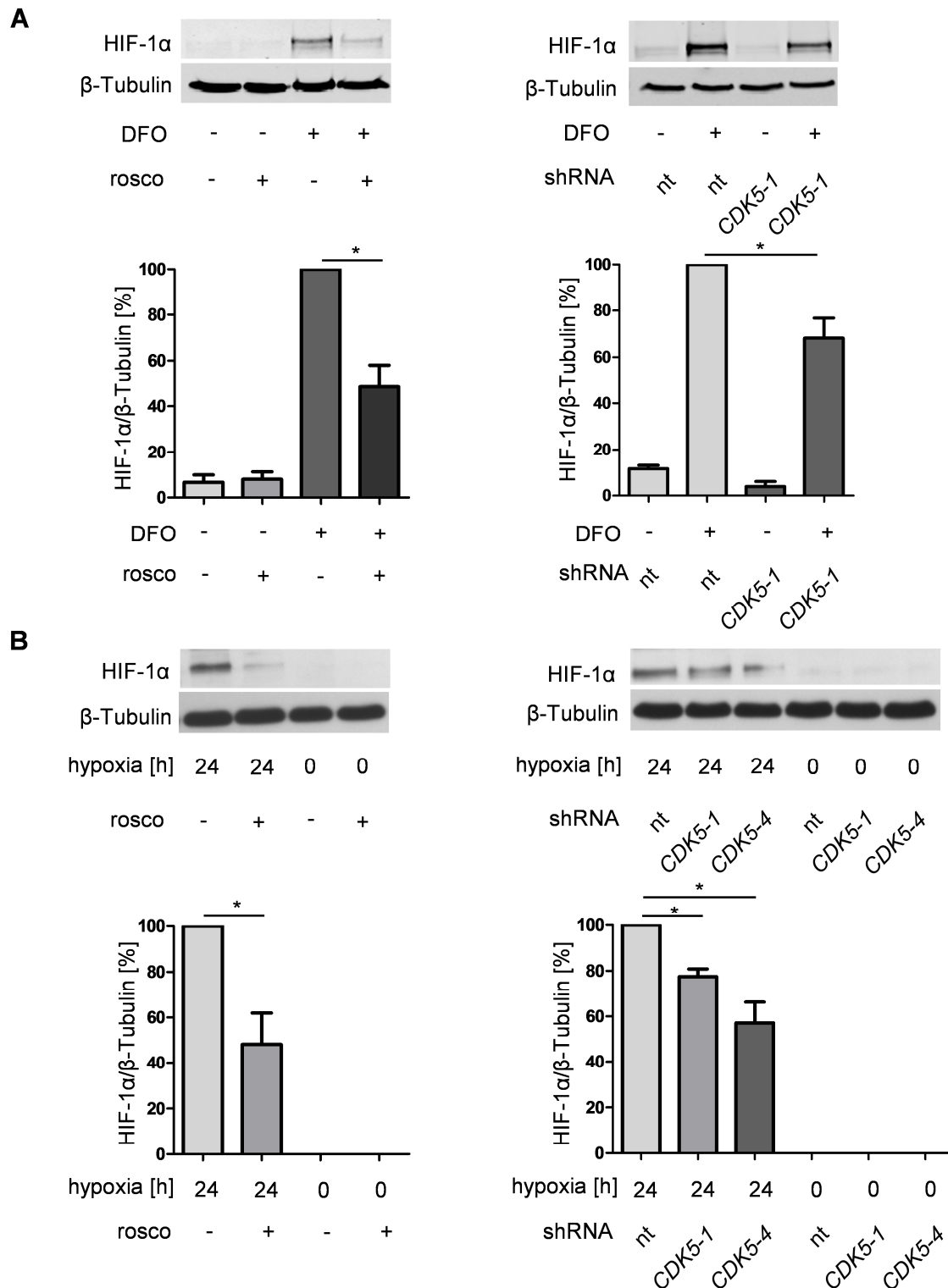


Figure 14: HIF-1α protein level correlates with CDK5 protein level in liver tumor cells.

(A) Immunoblots of HIF-1α, CDK5 and β-Tubulin in HUH7 lysates. CDK5 was either inhibited by roscovitine pretreatment for 30 minutes (30 μM) or stably down-regulated by *CDK5* shRNA. HUH7 cells were treated with 100 μM deferoxamine for six hours. The quantification is shown below the corresponding blot. One Way ANOVA on Newman-Keuls, * $p < 0.05$, $n = 3$. Error bars represent mean \pm SEM. **(B)** Immunoblots of either untreated or roscovitine pretreated HUH7 cells (30 μM, 30 minutes) or nt shRNA and *CDK5* shRNA HUH7 cells (two clones CDK5-1 and CDK5-4) are shown. Cells were incubated at 21% or 1% oxygen for 24 hours. Samples were probed for HIF-1α and β-Tubulin. The graphs below display the quantification of the immunoblots. One Way ANOVA on Newman-Keuls, * $p < 0.05$, $n = 3$. Error bars represent mean \pm SEM.

Additionally, under normoxic conditions P35/CDK5 overexpression led to an increase of HIF-1 α protein level (Fig. 15) again indicating a direct correlation between CDK5 and HIF-1 α in HUH7 cells.

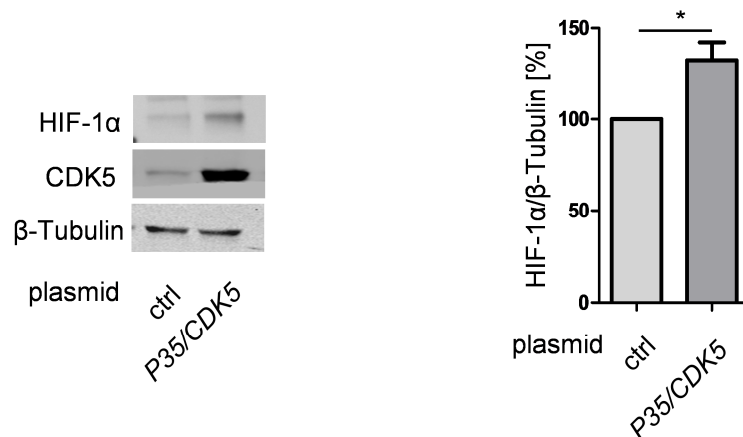


Figure 15: The protein level of HIF-1 α correlates with CDK5 protein level in liver tumor cells also under normoxia.

Immunoblot shows the protein level of HIF-1 α , CDK5 and β -Tubulin in HUH7 cells cultivated under normoxic conditions (21% oxygen). Cells were either transfected with a control plasmid or with a P35/CDK5 vector. One Way ANOVA on Newman-Keuls, * $p < 0.05$, $n = 3$. Error bars represent mean \pm SEM.

Furthermore, roscovitine treatment of HUH7 cells also led to a decrease of the DFO-induced protein level of HIF-2 α (Fig. 16).

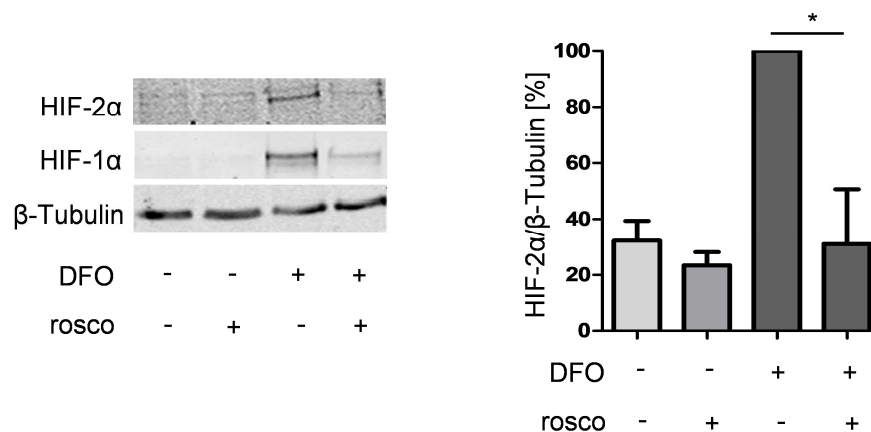


Figure 16: HIF-2 α protein level is reduced by CDK5 inhibition in liver tumor cells.

Immunoblot for HIF-2 α , HIF-1 α and β -Tubulin of HUH7 cells, either left untreated or treated with 30 μ M roscovitine, 30 minutes prior to deferoxamine treatment (100 μ M, six hours). Graph displays the quantification. One Way ANOVA on Newman-Keuls, * $p < 0.05$, $n = 3$. Error bars represent mean \pm SEM.

3.5 The transcription of HIF target genes and transcriptional activation of HIF is down-regulated in HCC cells upon CDK5 inhibition

Interestingly, it could be shown that not only the protein level of the transcription factor HIF-1 α is influenced by CDK5 inhibition, but also the transcription of its target genes *VEGFA* and *EphrinA1*. *VEGFA* and *EphrinA1* are both important modulators of angiogenic processes (1, 92) and *EphrinA1* has been shown to be highly upregulated in HCC, promoting cell growth of hepatocellular tumors (92). Both genes were significantly down-regulated upon CDK5 inhibition by roscovitine as well as in stable CDK5 knockdown clone 1 (Fig. 17).

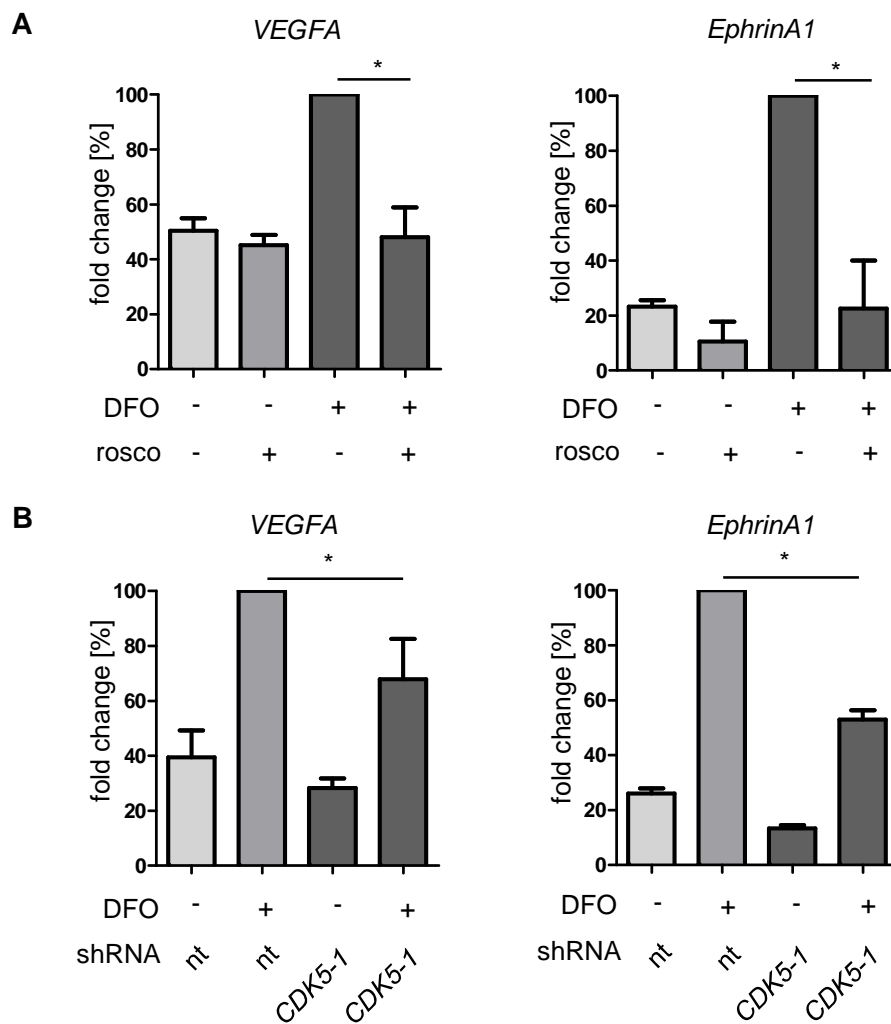


Figure 17: Pharmacological inhibition or distinct knockdown of CDK5 reduces the transcription of HIF target genes in liver tumor cells.

(A) Real-time PCR analysis of *VEGFA* and *EphrinA1* is shown. HUH7 cells were either left untreated or treated with 30 μ M roscovitine, 30 minutes prior to deferoxamine treatment (100 μ M, six hours). Graphs display the fold change in percent. One Way ANOVA on Newman-Keuls, * $p < 0.05$, $n = 3$. Error bars represent mean \pm SEM. **(B)** Real-time PCR of *VEGFA* and *EphrinA1* of nt shRNA HUH7 and CDK5 shRNA HUH7 cells is shown. Hypoxia was simulated with 100 μ M deferoxamine for six hours. Graphs display the fold change in percent. One Way ANOVA on Newman-Keuls, * $p < 0.05$, $n = 3$. Error bars represent mean \pm SEM.

Additionally, these data were confirmed in a luciferase assay which revealed a significant lower transcriptional activity of HIF-1 α in roscovitine treated cells and in CDK5 knockdown clone 1 in comparison to control (Fig. 18).

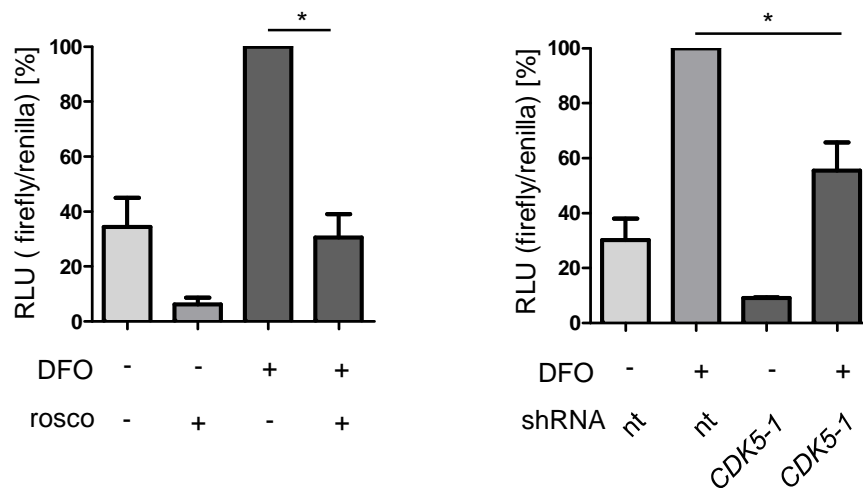


Figure 18: Pharmacological inhibition or distinct knockdown of CDK5 reduces the transcriptional activity of HIF-1 α in liver tumor cells.

Luciferase assay of HUH7 cells, transfected with a firefly luciferase vector *pGL4.27(HIF-REluc2P)* and a renilla luciferase vector *pGL4.74(hRLuc/TK)* is shown. CDK5 was either inhibited pharmacologically with roscovitine or down-regulated by distinct knockdown. The graphs show the relative light units (RLU) of firefly/renilla in percent. One Way ANOVA on Newman-Keuls, * $p < 0.05$, $n = 3$. Error bars represent mean \pm SEM.

3.6 CDK5 inhibition leads to a reduction of HIF-1 α *in vivo*

The influence of CDK5 inhibition on HIF-1 α *in vivo* was assessed in a HUH7 xenograft tumor model. Figure 19A shows a significant reduction in the area of HIF-1 α positive cells for tumors of mice treated with roscovitine. Accordingly, this effect could also be observed for tumors established from stable *CDK5* shRNA HUH7 cells (Fig. 19B).

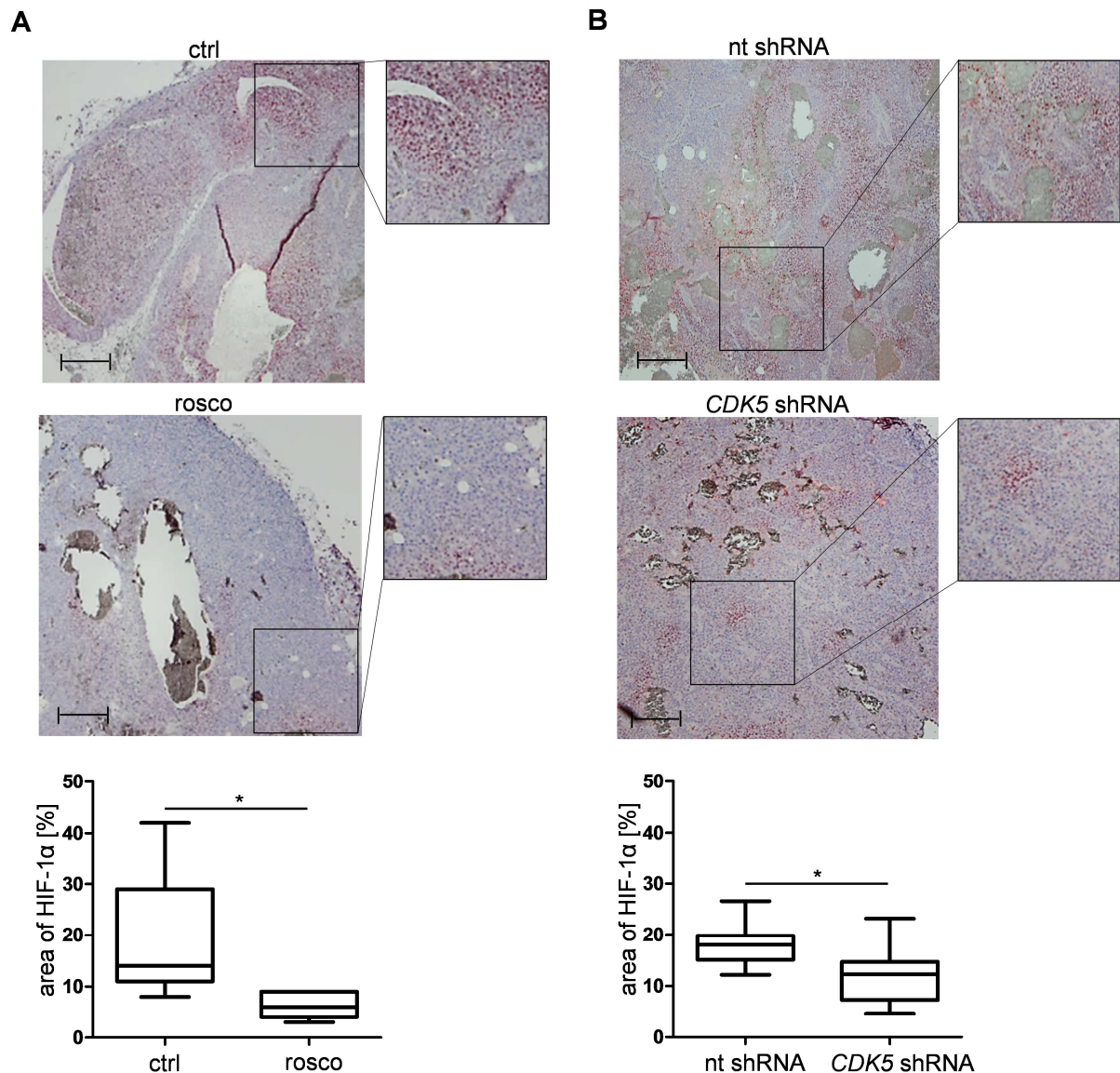


Figure 19: Pharmacological inhibition or distinct knockdown of CDK5 reduces the protein level of HIF-1 α in a HUH7 xenograft tumor model.

(A) Immunostaining of HIF-1 α (red) and haematoxylin (blue, nuclei) of HCC tumors grown in SCID mice either treated with solvents or roscovitine is shown. The graph shows the quantification of the tumor area with HIF-1 α positive cells of representative tissue sections from each tumor. Scale bars: 200 μ m. Non-parametric t-test on Mann-Whitney, * $p < 0.05$, $n = 8$. Whisker lines indicate maximum and minimum values. **(B)** Immunostaining of HIF-1 α (red) and haematoxylin (blue, nuclei) of tumors from nt shRNA HUH7 and *CDK5* shRNA HUH7 cells grown in SCID mice is shown. The graph shows the quantification of the tumor area with HIF-1 α positive cells of representative tissue sections from each tumor. Scale bars: 200 μ m. Non-parametric t-test on Mann-Whitney, * $p < 0.05$, $n = 11$. Whisker lines indicate maximum and minimum values.

3.7 CDK5 directly interacts with HIF-1 α preventing its proteasomal degradation

To get a better insight into how CDK5 might regulate angiogenesis in HCC via HIF-1 α , the focus was put on the interaction mechanism between CDK5 and the transcription factor. In a first step, co-immunoprecipitation experiments revealed a direct interaction between CDK5 and HIF-1 α (Fig. 20A). Furthermore, it could be shown that proteasome inhibition by MG132 totally rescues the effect of CDK5 inhibition on HIF-1 α (Fig. 20B).

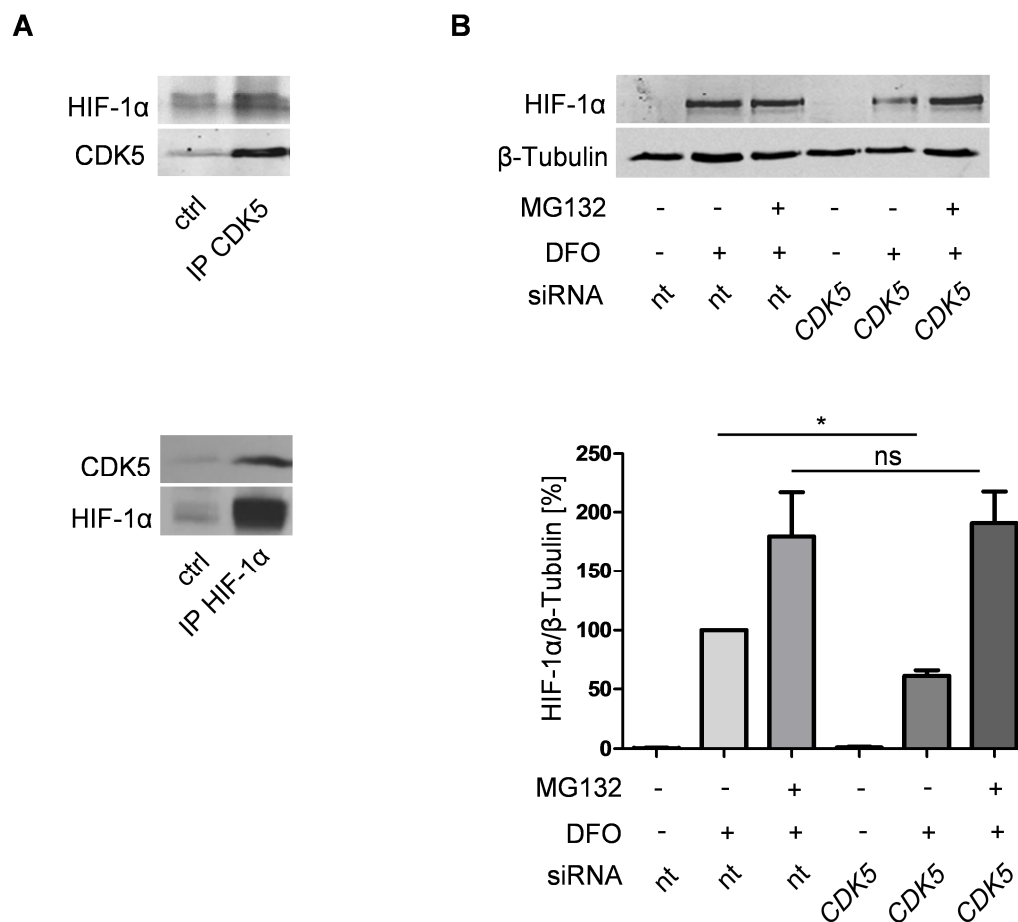


Figure 20: CDK5 directly interacts with HIF 1 α and protects it from proteasomal degradation.

(A) Co-immunoprecipitation of CDK5 and HIF-1 α in HUH7 cells, treated with 100 μ M deferoxamine for six hours. $n = 3$ **(B)** Immunoblot for HIF-1 α and β -Tubulin of lysates from HUVECs, either transfected with nt siRNA or *CDK5* siRNA is shown. Cells were left untreated or treated with 1 μ M of the proteasomal inhibitor MG132, 30 minutes prior to deferoxamine treatment (100 μ M, six hours). The quantification summarizes the ratio of HIF-1 α and β -Tubulin of three independent experiments. One Way ANOVA on Newman-Keuls, * $p < 0.05$, $n = 3$. Error bars represent mean \pm SEM.

3.8 CDK5 phosphorylates HIF-1 α at serine 687 leading to the stabilization of the transcription factor

The previous findings suggest that CDK5 directly phosphorylates HIF-1 α thereby promoting its stabilization. In fact, it was shown in this study in a kinase activity assay that recombinant P35/CDK5 phosphorylates recombinant HIF-1 α *in vitro* (Fig. 21).

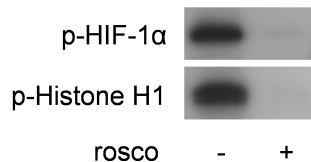


Figure 21: Recombinant P35/CDK5 phosphorylates recombinant HIF-1 α *in vitro*.

CDK5 kinase activity assay with recombinant P35/CDK5 and HIF-1 α is shown. The enzymatic transfer of ^{32}P from [$\gamma\text{-}^{32}\text{P}$] ATP to HIF-1 α was measured. P-Histone H1 served as control. Samples were either left untreated or treated with 100 μM roscovitine, $n = 3$.

Based on these data, mass spectrometry experiments were performed in order to find the CDK5 phosphorylation site responsible for HIF-1 α stabilization. Recombinant P35/CDK5 was incubated with recombinant HIF-1 α and ATP and the phosphorylations on HIF-1 α were analyzed. Interestingly, serine 687, which lies within the CDK5 motif aa 685-688, was identified to be phosphorylated by recombinant P35/CDK5. In a further mass spectrometry approach, HIF-1 α , immunoprecipitated from DFO treated HUH7 cells, also displayed a phosphorylation on serine 687 (Fig. 22A, mass spectra see supplementary data). To finally confirm the importance of phosphorylated serine 687 for the stability of HIF-1 α , point mutations of this site to either alanine (S687A) or glutamate (S687E) were generated in HA-HIF-1 α with site-directed mutagenesis (Fig. 22B, sequences see supplementary data). Alanine mutation was performed to prevent phosphorylation at S687 whereas glutamate mutation was used to simulate phosphorylation at this site.

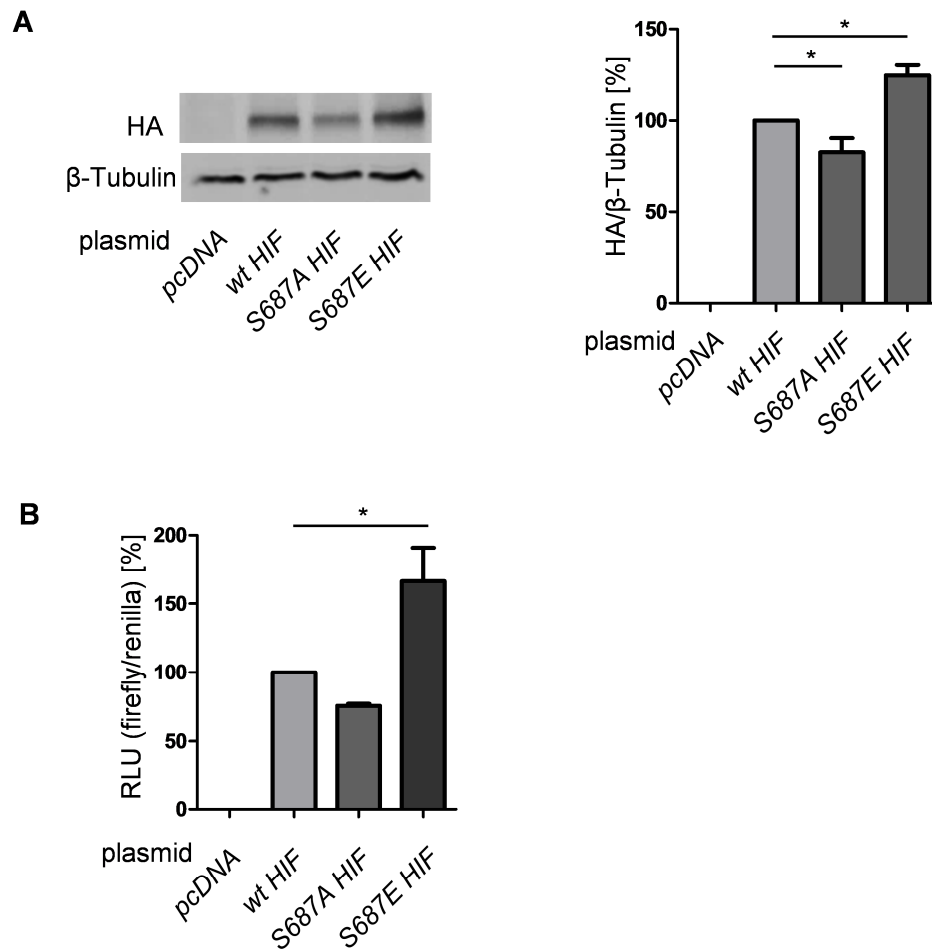


Figure 23: Phosphorylation of HIF-1 α at serine 687 by CDK5 promotes the stability of the transcription factor.

(A) Immunoblot of HUH7 cells either transfected with a control plasmid (*pcDNA*), *wt HA-HIF-1 α* , *S687A* or *S687E HA-HIF-1 α* is shown. Lysates were probed for HA and β -Tubulin. The graph displays the quantification of the immunoblots. One Way ANOVA on Newman-Keuls, * $p < 0.05$, $n = 3$. Error bars represent mean \pm SEM. **(B)** Dual-Luciferase assay of HUH7 cells either transfected with a control plasmid (*pcDNA*) or with *wt HA-HIF-1 α* , *S687A* or *S687E HA-HIF-1 α* is shown. Graph displays the RLU in percent. One Way ANOVA on Newman-Keuls, * $p < 0.05$, $n = 3$. Error bars represent mean \pm SEM.

DISCUSSION

4. DISCUSSION

4.1 Targeting HIFs via CDK5 inhibition in cancer therapy

In the present study the serine/threonine kinase CDK5 was identified as an interesting new target for anti-angiogenic therapy of HCC. CDK5 inhibition was demonstrated to lead to a significant decrease of the protein level of HIF-1 α and HIF-2 α as well as the transcription of HIF target genes such as *VEGFA* in endothelial and liver cancer cells. Upon CDK5 inhibition angiogenesis in different kinds of HCC mouse models was significantly reduced.

These results are consistent with the findings of Xie *et al.* who already showed a correlation of CDK5 and VEGF expression in pituitary adenomas (33). CDK5 is not only involved in several neuronal diseases as Alzheimer's disease (45) but also in different types of cancer like medullary thyroid carcinoma (30) and hepatocellular carcinoma (Ehrlich *et al.*, Journal of Hepatology, in revision). Haider *et al.* currently showed that CDK inhibitors BA12 and BP14 have strong antitumorigenic effects on hepatocellular carcinomas (50). In line with the findings of this study, the CDK inhibitor P276-00 has been demonstrated to inhibit HIF-1 α inducing G2/M arrest under hypoxia in prostate cancer cells also showing anti-angiogenic efficacy (93). Therefore, CDK5 inhibition might be of great interest as new therapeutic strategy, especially in the treatment of highly vascularized cancers.

4.2 Anti-angiogenic therapy as treatment strategy for hepatocellular carcinoma

Hypervascularity is a characteristic feature of hepatocellular carcinoma and an increase in microvascular density is associated with a poor prognosis (23). Angiogenesis is not only a fundamental step for tumor growth but also for invasion and metastasis (94). In this study, the efficacy of CDK5 inhibition on angiogenesis in different hepatocellular carcinoma mouse models was demonstrated. This is especially interesting, because hepatocellular carcinoma is the third leading cause of cancer-related death in the world (12) with a high resistance to systemic therapies even after aggressive local therapy. Therefore, there is an urgent need for new therapeutic options (95). In recent years anti-angiogenic therapy has become of increasing importance in preclinical and clinical assessments (23). Although there is evidence in pre-clinical studies, that anti-angiogenic therapy inhibits the growth of HCC (96), many of the results could not be confirmed in clinical trials (23). Currently used anti-

angiogenic drugs mainly target the VEGF pathway (1, 9). However, the process of angiogenesis does not depend on a single molecule. Zeng *et al.* even suggest a VEGF/angiopoietin-independent tumor blood supply in HCC (97). Additionally, there are several evasive mechanisms to anti-angiogenic VEGF therapy, like the activation of alternative pro-angiogenic pathways e.g. via hypoxia-inducible transcription factors (3).

4.3 Relevance of HIF-1 α and HIF-2 α inhibition in HCC

Hypoxia inducible factors are key players in cancer progression. They are activated under hypoxic conditions enhancing proliferation, angiogenesis, metastasis, chemoresistance and radioresistance of HCC (98). In this study, a significant down-regulation of the protein level of both subunits, HIF-1 α and HIF-2 α , as well as a reduction in the transcriptional activity was shown. Since it has already been demonstrated for hepatocellular tumor spheroids that knockdown of just one subunit, HIF-1 α or HIF-2 α , leads to the up-regulation of the other subunit, thereby eliminating survival advantages by dysregulating autophagy and apoptosis, targeting HIFs via CDK5 inhibition seems to be quite promising. Furthermore, a correlation between the oxygen-dependent subunit HIF-1 α and tumor size as well as a poor prognosis of HCC has already been shown (17). Moreover, Bangoura *et al.* showed a link between HIF-2 α expression and HCC tumor size, capsule infiltration, portal vein invasion and necrosis. In line with the findings of this study, they even suggest an involvement of HIF-2 α in HCC tumor angiogenesis, since HIF-2 α overexpression correlated with increased VEGF levels (77). Therefore, targeting HIF-1 α as well as HIF-2 α via CDK5 inhibition, could probably lead to a survival advantage of HCC patients, especially since HIF-1 α and HIF-2 α are both overexpressed in HCC (83). Concluding, HIFs are interesting candidates for HCC treatment and some HIF inhibitors are in clinical trials or already approved (82).

4.4 CDK5 phosphorylates HIF – the importance of post-translational modifications in the regulation of HIF stability and activation

Although an involvement of CDK5 in hypoxic signaling was already shown in mouse neuronal cells (51), the underlying mechanism behind was so far largely unknown. Post-translational modifications such as hydroxylation (53), ubiquitination (61), acetylation (99), S-nitrosylation (63) and also phosphorylation (62) have already been shown to influence HIF-1 half-life and its transcriptional activity. Furthermore an involvement of tyrosine and

serine/threonine kinases in phosphorylating HIF-1 α has previously been demonstrated, as their inhibition led to a decreased HIF expression, protein level and activity (100).

In this study it has been shown that CDK5 directly phosphorylates HIF-1 α at serine 687 in human liver cancer cells promoting its stabilization. Even though phosphorylation of HIF-1 α is known to influence its transcriptional activity, subcellular localization, protein-protein interaction and stability (79), only few phosphorylation sites responsible for HIF-1 α stabilization have been identified so far. Warfel *et al.* demonstrated that in colorectal cancer HIF-1 α is phosphorylated at serine 668 by CDK1 enhancing the stability of the transcription factor (101). Additionally, phosphorylation of HIF-1 α at serine 696 by the serine/threonine kinase ataxia telangiectasia mutated (ATM) has been shown to stabilize HIF-1 α down-regulating mTOR-complex1 signaling in pediatric solid tumors (102). These two phosphorylation sites lie within the inhibitory domain (aa 576-785) of HIF-1 α that inhibits transactivation of the transcription factor (64). Interestingly, the identified phosphorylation site at serine 687, which lies within the CDK5 consensus motif K/RT/SPXK (103, 104) in the inhibitory domain, is located in close proximity to these sites. The data of this study indicate that phosphorylation at serine 687 stabilizes HIF-1 α and induces its transcriptional activity thereby putatively overcoming the inhibitory function of this domain. Nevertheless, other post-transcriptional modifications certainly also contribute to HIF-1 α stabilization and it is still not clear, which mechanism is responsible for HIF-2 α stabilization. So there might be further phosphorylation sites yet to be identified.

4.5 Involvement of CDK2 in HIF stabilization

This study demonstrated that CDK2 might also be involved in the regulation of HIF protein levels and transcriptional activity in endothelial cells. In contrast to CDK5, this kinase is a main player in cell cycle control, especially in G1/S phase transition (105, 106). However, also a connection to HIF was already reported by Hubbi *et al.* (107). In line with the findings of this study, they showed that CDK2 enhances HIF-1 α transactivation function in the cancer cell lines HeLa and Hep3B. However, they revealed a decrease in HIF-1 α protein levels promoted by CDK2, explaining this contradictory mechanism based on two assumptions: cancer cells promote HIF-1 α degradation because the transcription factor induces cell cycle arrest during hypoxia (108) and cells try to compensate this by an increased HIF-1 target gene transcription (107). However, there are several reports underlining that this might be quite different in endothelial cells, because cells need to proliferate to ensure a sufficient blood supply of the tumor. Pro-proliferative mechanisms like the release of VEGF (109, 110) and insulin-like growth factor (111) are up-regulated in endothelial cells and anti-proliferative

substances like prostacyclin (112) and heparin sulphates (113, 114) have been demonstrated to be reduced under hypoxia. Since CDK inhibitors developed so far target at least both kinases, CDK2 and CDK5, due to their low specificity, the effect on HIF by pharmacological CDK inhibition might even be enhanced.

4.6 CDK5 inhibitors as therapeutic options in HCC therapy

Concerning cancer therapy, roscovitine (Seliciclib, CYC202), an orally available CDK inhibitor, is already undergoing clinical phase IIb trials, showing an increased overall survival for patients with non-small cell lung cancer (Cyclacel Press Release December 21, 2010). However, like most kinase inhibitors, roscovitine targets the ATP binding site of kinases, therefore being not very specific. A new approach would be to address CDK5 activators. For neurons Kesavapany *et al.* already demonstrated the positive effect of the CDK5 inhibitory peptide CIP on neuronal survival. CIP results from a further truncation of P35 (aa 54-279), which selectively targets P25/CDK5 interaction and thus prevents CDK5 hyperactivation. A deregulation of CDK5 by interaction with P25 and the associated abnormal phosphorylation of cytoskeletal proteins, is one of the hallmarks of many neurodegenerative diseases (115). In brain it has already been demonstrated, that *in vitro* endothelial cell angiogenesis is increased by shifting the balance between P35/CDK5 and P25/CDK5 signaling towards P35 (116). However, it is not clear so far, what role CDK5 deregulation plays during angiogenesis outside the brain and the role of P25/P35 as well as other putative activators of CDK5 in the endothelium are still to be identified.

Since sorafenib is the only available oral systemic treatment for advanced stage HCC patients so far (9), new therapeutic agents are needed. Recently, a novel oral selective mesenchymal-epithelial transition (MET) inhibitor, Tivantinib, has been evaluated in a phase II study, showing antitumor activity in HCC as monotherapy as well as in combination with sorafenib (117). Interestingly, Liu *et al.* showed that in HCC, the homeobox protein PROX1 promotes HIF-1 α transcription and influences its stability finally inducing epithelial-mesenchymal transition (EMT) response (118). Consequently, targeting HIFs via CDK5 inhibitors might not only affect angiogenesis in HCC, but putatively also influences the formation of metastases.

4.7 Conclusion and future perspectives

In summary, the observations of this study provided novel insight into the regulation of angiogenesis in human endothelial and liver cancer cells. There is compelling evidence that CDK5 is involved in hypoxic signaling by directly stabilizing HIF-1 α and HIF-2 α , thus promoting the formation of blood vessels. Together with the findings of Ehrlich *et al.* (Journal of Hepatology, in revision) who showed that CDK5 inhibition leads to a reduced HCC proliferation and clonogenic survival and also reveals *in vivo* efficacy in a HCC xenograft mouse model, the importance of CDK5 as a new therapeutic target is demonstrated.

This underlines the potential of CDK5 inhibitors as anti-cancer drugs for HCC treatment. The combination with other anti-angiogenic agents might even improve their efficiency and therefore clinical outcome for patients (82). Since HIF-1 α activity is not only associated with cancer development but also leads to the pathogenesis of several other diseases such as retinopathy, pulmonary arterial hypertension as well as traumatic shock and obstructive sleep apnea (119), CDK5 might be of broad interest as a pharmacologically accessible therapeutic target with a surprising mode of action.

SUMMARY

5. SUMMARY

Recently, the cyclin-dependent kinase 5 (CDK5), a serine/threonine kinase, has been identified to have a role in the regulation of angiogenesis. To test the impact of this finding on tumor biology, the involvement of CDK5 in angiogenesis of liver cancer was investigated in this study, since hepatocellular carcinoma (HCC) is one of the most vascularized solid tumors. Pharmacological or genetic inhibition of CDK5 in endothelial or HCC cells led to a reduction of HIF-1 α *in vitro* and *in vivo*. Furthermore, the CDK5 inhibitor roscovitine significantly reduced the HIF-2 α protein level *in vitro*. Consequently, transcription of HIF target genes (*VEGFA*, *VEGFR1*, *EphrinA1*) was decreased. Mass spectrometry revealed that CDK5 directly phosphorylated HIF-1 α at serine 687, resulting in a stabilization of the transcription factor. Mutation studies confirmed the functional relevance of this phosphorylation site for HIF-1 α stability. As *in vivo* proof, vascular density was decreased in different kinds of murine HCC models by pharmacological CDK5 inhibition. Thus, HIF was identified as a new substrate of CDK5 in endothelial and liver cancer cells.

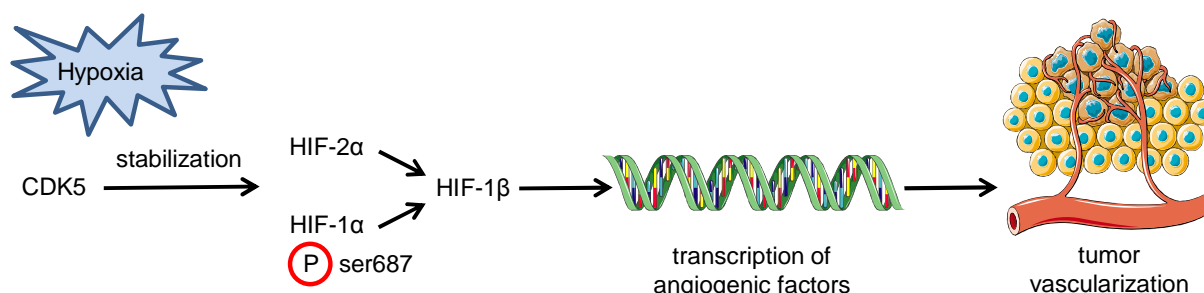


Figure 24: CDK5 stabilizes HIF, promoting angiogenesis in HCC.

Concluding, this study underlines the potential of CDK5 inhibitors as anti-angiogenic cancer therapeutics. Besides HCC, where high HIF levels correlate with poor prognosis, the pathogenesis of other diseases like retinopathy or pulmonary arterial hypertension is also caused by a high HIF activity. Therefore, targeting CDK5 might be of considerable general interest as a novel therapeutic option to address HIF-1 α related diseases.

REFERENCES

6. REFERENCES

1. Giuliano S, and Pages G. Mechanisms of resistance to anti-angiogenesis therapies. *Biochimie*. 2013;95(6):1110-9.
2. Folkman J. Angiogenesis: an organizing principle for drug discovery? *Nature reviews Drug discovery*. 2007;6(4):273-86.
3. Bergers G, and Hanahan D. Modes of resistance to anti-angiogenic therapy. *Nature reviews Cancer*. 2008;8(8):592-603.
4. Yue PY, Mak NK, Cheng YK, Leung KW, Ng TB, Fan DT, Yeung HW, and Wong RN. Pharmacogenomics and the Yin/Yang actions of ginseng: anti-tumor, angiomodulating and steroid-like activities of ginsenosides. *Chinese medicine*. 2007;2(6).
5. Folkman J, and Shing Y. Angiogenesis. *The Journal of biological chemistry*. 1992;267(16):10931-4.
6. Risau W. Mechanisms of angiogenesis. *Nature*. 1997;386(6626):671-4.
7. Folkman J, and Klagsbrun M. Angiogenic factors. *Science*. 1987;235(4787):442-7.
8. Chung AS, Lee J, and Ferrara N. Targeting the tumour vasculature: insights from physiological angiogenesis. *Nature reviews Cancer*. 2010;10(7):505-14.
9. Wrzesinski SH, Taddei TH, and Strazzabosco M. Systemic therapy in hepatocellular carcinoma. *Clinics in liver disease*. 2011;15(2):423-41, vii-x.
10. Ebos JM, Lee CR, Christensen JG, Mutsaers AJ, and Kerbel RS. Multiple circulating proangiogenic factors induced by sunitinib malate are tumor-independent and correlate with antitumor efficacy. *Proceedings of the National Academy of Sciences of the United States of America*. 2007;104(43):17069-74.
11. Lu KV, and Bergers G. Mechanisms of evasive resistance to anti-VEGF therapy in glioblastoma. *CNS oncology*. 2013;2(1):49-65.
12. Ferlay J, Shin HR, Bray F, Forman D, Mathers C, and Parkin DM. Estimates of worldwide burden of cancer in 2008: GLOBOCAN 2008. *International journal of cancer Journal international du cancer*. 2010;127(12):2893-917.
13. Parkin DM, Bray F, Ferlay J, and Pisani P. Estimating the world cancer burden: Globocan 2000. *International journal of cancer Journal international du cancer*. 2001;94(2):153-6.
14. El-Serag HB, Davila JA, Petersen NJ, and McGlynn KA. The continuing increase in the incidence of hepatocellular carcinoma in the United States: an update. *Annals of internal medicine*. 2003;139(10):817-23.
15. Thomas MB, and Zhu AX. Hepatocellular carcinoma: the need for progress. *Journal of clinical oncology : official journal of the American Society of Clinical Oncology*. 2005;23(13):2892-9.
16. Poon RT, Fan ST, Lo CM, Ng IO, Liu CL, Lam CM, and Wong J. Improving survival results after resection of hepatocellular carcinoma: a prospective study of 377 patients over 10 years. *Annals of surgery*. 2001;234(1):63-70.
17. Li S, Yao D, Wang L, Wu W, Qiu L, Yao M, Yao N, Zhang H, Yu D, and Ni Q. Expression characteristics of hypoxia-inducible factor-1alpha and its clinical values in diagnosis and prognosis of hepatocellular carcinoma. *Hepatitis monthly*. 2011;11(10):821-8.
18. Miura H, Miyazaki T, Kuroda M, Oka T, Machinami R, Kodama T, Shibuya M, Makuuchi M, Yazaki Y, and Ohnishi S. Increased expression of vascular endothelial growth factor in human hepatocellular carcinoma. *Journal of hepatology*. 1997;27(5):854-61.
19. Poon RT, Ho JW, Tong CS, Lau C, Ng IO, and Fan ST. Prognostic significance of serum vascular endothelial growth factor and endostatin in patients with hepatocellular carcinoma. *The British journal of surgery*. 2004;91(10):1354-60.
20. El-Assal ON, Yamanoi A, Ono T, Kohno H, and Nagasue N. The clinicopathological significance of heparanase and basic fibroblast growth factor expressions in hepatocellular carcinoma. *Clinical cancer research : an official journal of the American Association for Cancer Research*. 2001;7(5):1299-305.

21. Poon RT, Ng IO, Lau C, Yu WC, Fan ST, and Wong J. Correlation of serum basic fibroblast growth factor levels with clinicopathologic features and postoperative recurrence in hepatocellular carcinoma. *American journal of surgery*. 2001;182(3):298-304.
22. Pang RW, and Poon RT. From molecular biology to targeted therapies for hepatocellular carcinoma: the future is now. *Oncology*. 2007;72 Suppl 1(30-44).
23. Ribatti D, Vacca A, Nico B, Sansonno D, and Dammacco F. Angiogenesis and anti-angiogenesis in hepatocellular carcinoma. *Cancer treatment reviews*. 2006;32(6):437-44.
24. Lew J, Beaudette K, Litwin CM, and Wang JH. Purification and characterization of a novel proline-directed protein kinase from bovine brain. *The Journal of biological chemistry*. 1992;267(19):13383-90.
25. Liebl J, Furst R, Vollmar AM, and Zahler S. Twice switched at birth: cell cycle-independent roles of the "neuron-specific" cyclin-dependent kinase 5 (Cdk5) in non-neuronal cells. *Cellular signalling*. 2011;23(11):1698-707.
26. Zukerberg LR, Patrick GN, Nikolic M, Humbert S, Wu CL, Lanier LM, Gertler FB, Vidal M, Van Etten RA, and Tsai LH. Cables links Cdk5 and c-Abl and facilitates Cdk5 tyrosine phosphorylation, kinase upregulation, and neurite outgrowth. *Neuron*. 2000;26(3):633-46.
27. Sasaki Y, Cheng C, Uchida Y, Nakajima O, Ohshima T, Yagi T, Taniguchi M, Nakayama T, Kishida R, Kudo Y, et al. Fyn and Cdk5 mediate semaphorin-3A signaling, which is involved in regulation of dendrite orientation in cerebral cortex. *Neuron*. 2002;35(5):907-20.
28. Feldmann G, Mishra A, Hong SM, Bisht S, Strock CJ, Ball DW, Goggins M, Maitra A, and Nelkin BD. Inhibiting the cyclin-dependent kinase CDK5 blocks pancreatic cancer formation and progression through the suppression of Ras-Ral signaling. *Cancer research*. 2010;70(11):4460-9.
29. Demelash A, Rudrabhatla P, Pant HC, Wang X, Amin ND, McWhite CD, Naizhen X, and Linnoila RI. Achaete-scute homologue-1 (ASH1) stimulates migration of lung cancer cells through Cdk5/p35 pathway. *Molecular biology of the cell*. 2012;23(15):2856-66.
30. Pozo K, Castro-Rivera E, Tan C, Plattner F, Schwach G, Siegl V, Meyer D, Guo A, Gundara J, Mettlach G, et al. The role of Cdk5 in neuroendocrine thyroid cancer. *Cancer cell*. 2013;24(4):499-511.
31. Liebl J, Weitensteiner SB, Vereb G, Takacs L, Furst R, Vollmar AM, and Zahler S. Cyclin-dependent kinase 5 regulates endothelial cell migration and angiogenesis. *The Journal of biological chemistry*. 2010;285(46):35932-43.
32. Sharma MR, Tuszyński GP, and Sharma MC. Angiostatin-induced inhibition of endothelial cell proliferation/apoptosis is associated with the down-regulation of cell cycle regulatory protein cdk5. *Journal of cellular biochemistry*. 2004;91(2):398-409.
33. Xie W, Wang H, He Y, Li D, Gong L, and Zhang Y. CDK5 and its activator P35 in normal pituitary and in pituitary adenomas: relationship to VEGF expression. *International journal of biological sciences*. 2014;10(2):192-9.
34. Cruz JC, Kim D, Moy LY, Dobbin MM, Sun X, Bronson RT, and Tsai LH. p25/cyclin-dependent kinase 5 induces production and intraneuronal accumulation of amyloid beta in vivo. *The Journal of neuroscience : the official journal of the Society for Neuroscience*. 2006;26(41):10536-41.
35. Cruz JC, and Tsai LH. Cdk5 deregulation in the pathogenesis of Alzheimer's disease. *Trends in molecular medicine*. 2004;10(9):452-8.
36. Sadleir KR, and Vassar R. Cdk5 protein inhibition and Abeta42 increase BACE1 protein level in primary neurons by a post-transcriptional mechanism: implications of CDK5 as a therapeutic target for Alzheimer disease. *The Journal of biological chemistry*. 2012;287(10):7224-35.
37. Wong AS, Lee RH, Cheung AY, Yeung PK, Chung SK, Cheung ZH, and Ip NY. Cdk5-mediated phosphorylation of endophilin B1 is required for induced autophagy in models of Parkinson's disease. *Nature cell biology*. 2011;13(5):568-79.
38. Anne SL, Saudou F, and Humbert S. Phosphorylation of huntingtin by cyclin-dependent kinase 5 is induced by DNA damage and regulates wild-type and mutant huntingtin toxicity in

- neurons. *The Journal of neuroscience : the official journal of the Society for Neuroscience*. 2007;27(27):7318-28.
39. Menn B, Bach S, Blevins TL, Campbell M, Meijer L, and Timsit S. Delayed treatment with systemic (S)-roscovitine provides neuroprotection and inhibits in vivo CDK5 activity increase in animal stroke models. *PloS one*. 2010;5(8):e12117.
 40. Pareek TK, and Kulkarni AB. Cdk5: a new player in pain signaling. *Cell cycle*. 2006;5(6):585-8.
 41. Utreras E, Futatsugi A, Rudrabhatla P, Keller J, Iadarola MJ, Pant HC, and Kulkarni AB. Tumor necrosis factor-alpha regulates cyclin-dependent kinase 5 activity during pain signaling through transcriptional activation of p35. *The Journal of biological chemistry*. 2009;284(4):2275-84.
 42. Wei FY, Nagashima K, Ohshima T, Saheki Y, Lu YF, Matsushita M, Yamada Y, Mikoshiba K, Seino Y, Matsui H, et al. Cdk5-dependent regulation of glucose-stimulated insulin secretion. *Nature medicine*. 2005;11(10):1104-8.
 43. Vesely J, Havlicek L, Strnad M, Blow JJ, Donella-Deana A, Pinna L, Letham DS, Kato J, Detivaud L, Leclerc S, et al. Inhibition of cyclin-dependent kinases by purine analogues. *European journal of biochemistry / FEBS*. 1994;224(2):771-86.
 44. Meijer L, Borgne A, Mulner O, Chong JP, Blow JJ, Inagaki N, Inagaki M, Delcros JG, and Moulinoux JP. Biochemical and cellular effects of roscovitine, a potent and selective inhibitor of the cyclin-dependent kinases cdc2, cdk2 and cdk5. *European journal of biochemistry / FEBS*. 1997;243(1-2):527-36.
 45. Demange L, Abdellah FN, Lozach O, Ferandin Y, Gresh N, Meijer L, and Galons H. Potent inhibitors of CDK5 derived from roscovitine: synthesis, biological evaluation and molecular modelling. *Bioorganic & medicinal chemistry letters*. 2013;23(1):125-31.
 46. Knockaert M, Greengard P, and Meijer L. Pharmacological inhibitors of cyclin-dependent kinases. *Trends in pharmacological sciences*. 2002;23(9):417-25.
 47. Hoessel R, Leclerc S, Endicott JA, Nobel ME, Lawrie A, Tunnah P, Leost M, Damiens E, Marie D, Marko D, et al. Indirubin, the active constituent of a Chinese antileukaemia medicine, inhibits cyclin-dependent kinases. *Nature cell biology*. 1999;1(1):60-7.
 48. Mettey Y, Gompel M, Thomas V, Garnier M, Leost M, Ceballos-Picot I, Noble M, Endicott J, Vierfond JM, and Meijer L. Aloisines, a new family of CDK/GSK-3 inhibitors. SAR study, crystal structure in complex with CDK2, enzyme selectivity, and cellular effects. *Journal of medicinal chemistry*. 2003;46(2):222-36.
 49. Zaharevitz DW, Gussio R, Leost M, Senderowicz AM, Lahusen T, Kunick C, Meijer L, and Sausville EA. Discovery and initial characterization of the paullones, a novel class of small-molecule inhibitors of cyclin-dependent kinases. *Cancer research*. 1999;59(11):2566-9.
 50. Haider C, Grubinger M, Reznickova E, Weiss TS, Rotheneder H, Miklos W, Berger W, Jorda R, Zatloukal M, Gucky T, et al. Novel inhibitors of cyclin-dependent kinases combat hepatocellular carcinoma without inducing chemoresistance. *Molecular cancer therapeutics*. 2013;12(10):1947-57.
 51. Antoniou X, Gassmann M, and Ogunshola OO. Cdk5 interacts with Hif-1alpha in neurons: a new hypoxic signalling mechanism? *Brain research*. 2011;1381(1-10).
 52. Jiang BH, Rue E, Wang GL, Roe R, and Semenza GL. Dimerization, DNA binding, and transactivation properties of hypoxia-inducible factor 1. *The Journal of biological chemistry*. 1996;271(30):17771-8.
 53. Ke Q, and Costa M. Hypoxia-inducible factor-1 (HIF-1). *Molecular pharmacology*. 2006;70(5):1469-80.
 54. Jewell UR, Kvietikova I, Scheid A, Bauer C, Wenger RH, and Gassmann M. Induction of HIF-1alpha in response to hypoxia is instantaneous. *FASEB journal : official publication of the Federation of American Societies for Experimental Biology*. 2001;15(7):1312-4.
 55. Wang GL, Jiang BH, Rue EA, and Semenza GL. Hypoxia-inducible factor 1 is a basic-helix-loop-helix-PAS heterodimer regulated by cellular O2 tension. *Proceedings of the National Academy of Sciences of the United States of America*. 1995;92(12):5510-4.

56. Wang GL, and Semenza GL. Purification and characterization of hypoxia-inducible factor 1. *The Journal of biological chemistry*. 1995;270(3):1230-7.
57. Luo D, Wang Z, Wu J, Jiang C, and Wu J. The role of hypoxia inducible factor-1 in hepatocellular carcinoma. *BioMed research international*. 2014;2014(409272).
58. Pugh CW, O'Rourke JF, Nagao M, Gleadle JM, and Ratcliffe PJ. Activation of hypoxia-inducible factor-1; definition of regulatory domains within the alpha subunit. *The Journal of biological chemistry*. 1997;272(17):11205-14.
59. Ema M, Hirota K, Mimura J, Abe H, Yodoi J, Sogawa K, Poellinger L, and Fujii-Kuriyama Y. Molecular mechanisms of transcription activation by HLF and HIF1alpha in response to hypoxia: their stabilization and redox signal-induced interaction with CBP/p300. *The EMBO journal*. 1999;18(7):1905-14.
60. Kallio PJ, Okamoto K, O'Brien S, Carrero P, Makino Y, Tanaka H, and Poellinger L. Signal transduction in hypoxic cells: inducible nuclear translocation and recruitment of the CBP/p300 coactivator by the hypoxia-inducible factor-1alpha. *The EMBO journal*. 1998;17(22):6573-86.
61. Brahimi-Horn C, Mazure N, and Pouyssegur J. Signalling via the hypoxia-inducible factor-1alpha requires multiple posttranslational modifications. *Cellular signalling*. 2005;17(1):1-9.
62. Xu D, Yao Y, Lu L, Costa M, and Dai W. Plk3 functions as an essential component of the hypoxia regulatory pathway by direct phosphorylation of HIF-1alpha. *The Journal of biological chemistry*. 2010;285(50):38944-50.
63. Li F, Sonveaux P, Rabbani ZN, Liu S, Yan B, Huang Q, Vujaskovic Z, Dewhirst MW, and Li CY. Regulation of HIF-1alpha stability through S-nitrosylation. *Molecular cell*. 2007;26(1):63-74.
64. Jiang BH, Zheng JZ, Leung SW, Roe R, and Semenza GL. Transactivation and inhibitory domains of hypoxia-inducible factor 1alpha. Modulation of transcriptional activity by oxygen tension. *The Journal of biological chemistry*. 1997;272(31):19253-60.
65. Semenza GL. Hydroxylation of HIF-1: oxygen sensing at the molecular level. *Physiology*. 2004;19(176-82).
66. Ema M, Taya S, Yokotani N, Sogawa K, Matsuda Y, and Fujii-Kuriyama Y. A novel bHLH-PAS factor with close sequence similarity to hypoxia-inducible factor 1alpha regulates the VEGF expression and is potentially involved in lung and vascular development. *Proceedings of the National Academy of Sciences of the United States of America*. 1997;94(9):4273-8.
67. Tian H, Hammer RE, Matsumoto AM, Russell DW, and McKnight SL. The hypoxia-responsive transcription factor EPAS1 is essential for catecholamine homeostasis and protection against heart failure during embryonic development. *Genes & development*. 1998;12(21):3320-4.
68. Tian H, McKnight SL, and Russell DW. Endothelial PAS domain protein 1 (EPAS1), a transcription factor selectively expressed in endothelial cells. *Genes & development*. 1997;11(1):72-82.
69. Wiesener MS, Jurgensen JS, Rosenberger C, Scholze CK, Horstrup JH, Warnecke C, Mandriota S, Bechmann I, Frei UA, Pugh CW, et al. Widespread hypoxia-inducible expression of HIF-2alpha in distinct cell populations of different organs. *FASEB journal : official publication of the Federation of American Societies for Experimental Biology*. 2003;17(2):271-3.
70. Heikkila M, Pasanen A, Kivirikko KI, and Myllyharju J. Roles of the human hypoxia-inducible factor (HIF)-3alpha variants in the hypoxia response. *Cellular and molecular life sciences : CMLS*. 2011;68(23):3885-901.
71. Tanaka T, Wiesener M, Bernhardt W, Eckardt KU, and Warnecke C. The human HIF (hypoxia-inducible factor)-3alpha gene is a HIF-1 target gene and may modulate hypoxic gene induction. *The Biochemical journal*. 2009;424(1):143-51.
72. Maynard MA, Evans AJ, Shi W, Kim WY, Liu FF, and Ohh M. Dominant-negative HIF-3 alpha 4 suppresses VHL-null renal cell carcinoma progression. *Cell cycle*. 2007;6(22):2810-6.
73. Rankin EB, and Giaccia AJ. The role of hypoxia-inducible factors in tumorigenesis. *Cell death and differentiation*. 2008;15(4):678-85.

74. Faller DV. Endothelial cell responses to hypoxic stress. *Clinical and experimental pharmacology & physiology*. 1999;26(1):74-84.
75. Fischer C, Mazzone M, Jonckx B, and Carmeliet P. FLT1 and its ligands VEGFB and PlGF: drug targets for anti-angiogenic therapy? *Nature reviews Cancer*. 2008;8(12):942-56.
76. Namiki A, Brogi E, Kearney M, Kim EA, Wu T, Couffignal T, Varticovski L, and Isner JM. Hypoxia induces vascular endothelial growth factor in cultured human endothelial cells. *The Journal of biological chemistry*. 1995;270(52):31189-95.
77. Bangoura G, Liu ZS, Qian Q, Jiang CQ, Yang GF, and Jing S. Prognostic significance of HIF-2alpha/EPAS1 expression in hepatocellular carcinoma. *World journal of gastroenterology : WJG*. 2007;13(23):3176-82.
78. Xie H, Song J, Liu K, Ji H, Shen H, Hu S, Yang G, Du Y, Zou X, Jin H, et al. The expression of hypoxia-inducible factor-1alpha in hepatitis B virus-related hepatocellular carcinoma: correlation with patients' prognosis and hepatitis B virus X protein. *Digestive diseases and sciences*. 2008;53(12):3225-33.
79. Dimova EY, Michiels C, and Kietzmann T. Kinases as upstream regulators of the HIF system: their emerging potential as anti-cancer drug targets. *Current pharmaceutical design*. 2009;15(33):3867-77.
80. Xia Y, Choi HK, and Lee K. Recent advances in hypoxia-inducible factor (HIF)-1 inhibitors. *European journal of medicinal chemistry*. 2012;49(24-40).
81. Sadri N, and Zhang PJ. Hypoxia-inducible factors: mediators of cancer progression; prognostic and therapeutic targets in soft tissue sarcomas. *Cancers*. 2013;5(2):320-33.
82. Semenza GL. Hypoxia-inducible factors: mediators of cancer progression and targets for cancer therapy. *Trends in pharmacological sciences*. 2012;33(4):207-14.
83. Menrad H, Werno C, Schmid T, Copanaki E, Deller T, Dehne N, and Brune B. Roles of hypoxia-inducible factor-1alpha (HIF-1alpha) versus HIF-2alpha in the survival of hepatocellular tumor spheroids. *Hepatology*. 2010;51(6):2183-92.
84. Roxburgh P, and Evans TR. Systemic therapy of hepatocellular carcinoma: are we making progress? *Advances in therapy*. 2008;25(11):1089-104.
85. Zatloukal M, Jorda R, Gucky T, Reznickova E, Voller J, Pospisil T, Malinkova V, Adamcova H, Krystof V, and Strnad M. Synthesis and in vitro biological evaluation of 2,6,9-trisubstituted purines targeting multiple cyclin-dependent kinases. *European journal of medicinal chemistry*. 2013;61(61-72).
86. van den Heuvel S, and Harlow E. Distinct roles for cyclin-dependent kinases in cell cycle control. *Science*. 1993;262(5142):2050-4.
87. Baker SJ, Markowitz S, Fearon ER, Willson JK, and Vogelstein B. Suppression of human colorectal carcinoma cell growth by wild-type p53. *Science*. 1990;249(4971):912-5.
88. Kondo K, Klco J, Nakamura E, Lechpammer M, and Kaelin WG, Jr. Inhibition of HIF is necessary for tumor suppression by the von Hippel-Lindau protein. *Cancer cell*. 2002;1(3):237-46.
89. Pfaffl MW. A new mathematical model for relative quantification in real-time RT-PCR. *Nucleic acids research*. 2001;29(9):e45.
90. Tardio JC. CD34-reactive tumors of the skin. An updated review of an ever-growing list of lesions. *Journal of cutaneous pathology*. 2009;36(1):89-102.
91. Liao D, and Johnson RS. Hypoxia: a key regulator of angiogenesis in cancer. *Cancer metastasis reviews*. 2007;26(2):281-90.
92. Iida H, Honda M, Kawai HF, Yamashita T, Shiota Y, Wang BC, Miao H, and Kaneko S. Ephrin-A1 expression contributes to the malignant characteristics of {alpha}-fetoprotein producing hepatocellular carcinoma. *Gut*. 2005;54(6):843-51.
93. Manohar SM, Padgaonkar AA, Jalota-Badhwari A, Rao SV, and Joshi KS. Cyclin-dependent kinase inhibitor, P276-00, inhibits HIF-1alpha and induces G2/M arrest under hypoxia in prostate cancer cells. *Prostate cancer and prostatic diseases*. 2012;15(1):15-27.

94. Ribatti D, Vacca A, and Dammacco F. The role of the vascular phase in solid tumor growth: a historical review. *Neoplasia*. 1999;1(4):293-302.
95. Zhu AX, Duda DG, Sahani DV, and Jain RK. HCC and angiogenesis: possible targets and future directions. *Nature reviews Clinical oncology*. 2011;8(5):292-301.
96. Pang R, and Poon RT. Angiogenesis and antiangiogenic therapy in hepatocellular carcinoma. *Cancer letters*. 2006;242(2):151-67.
97. Zeng W, Gouw AS, van den Heuvel MC, Zwiers PJ, Zondervan PE, Poppema S, Zhang N, Platteel I, de Jong KP, and Molema G. The angiogenic makeup of human hepatocellular carcinoma does not favor vascular endothelial growth factor/angiopoietin-driven sprouting neovascularization. *Hepatology*. 2008;48(5):1517-27.
98. Wu XZ, Xie GR, and Chen D. Hypoxia and hepatocellular carcinoma: The therapeutic target for hepatocellular carcinoma. *Journal of gastroenterology and hepatology*. 2007;22(8):1178-82.
99. Jeong JW, Bae MK, Ahn MY, Kim SH, Sohn TK, Bae MH, Yoo MA, Song EJ, Lee KJ, and Kim KW. Regulation and destabilization of HIF-1alpha by ARD1-mediated acetylation. *Cell*. 2002;111(5):709-20.
100. Wang GL, Jiang BH, and Semenza GL. Effect of protein kinase and phosphatase inhibitors on expression of hypoxia-inducible factor 1. *Biochemical and biophysical research communications*. 1995;216(2):669-75.
101. Warfel NA, Dolloff NG, Dicker DT, Malysz J, and El-Deiry WS. CDK1 stabilizes HIF-1alpha via direct phosphorylation of Ser668 to promote tumor growth. *Cell cycle*. 2013;12(23):3689-701.
102. Cam H, Easton JB, High A, and Houghton PJ. mTORC1 signaling under hypoxic conditions is controlled by ATM-dependent phosphorylation of HIF-1alpha. *Molecular cell*. 2010;40(4):509-20.
103. Shetty KT, Link WT, and Pant HC. cdc2-like kinase from rat spinal cord specifically phosphorylates KSPXK motifs in neurofilament proteins: isolation and characterization. *Proceedings of the National Academy of Sciences of the United States of America*. 1993;90(14):6844-8.
104. Grant P, Sharma P, and Pant HC. Cyclin-dependent protein kinase 5 (Cdk5) and the regulation of neurofilament metabolism. *European journal of biochemistry / FEBS*. 2001;268(6):1534-46.
105. Saha P, Chen J, Thome KC, Lawlis SJ, Hou ZH, Hendricks M, Parvin JD, and Dutta A. Human CDC6/Cdc18 associates with Orc1 and cyclin-cdk and is selectively eliminated from the nucleus at the onset of S phase. *Molecular and cellular biology*. 1998;18(5):2758-67.
106. Lei M, Kawasaki Y, Young MR, Kihara M, Sugino A, and Tye BK. Mcm2 is a target of regulation by Cdc7-Dbf4 during the initiation of DNA synthesis. *Genes & development*. 1997;11(24):3365-74.
107. Hubbi ME, Gilkes DM, Hu H, Kshitiz, Ahmed I, and Semenza GL. Cyclin-dependent kinases regulate lysosomal degradation of hypoxia-inducible factor 1alpha to promote cell-cycle progression. *Proceedings of the National Academy of Sciences of the United States of America*. 2014;111(32):E3325-34.
108. Goda N, Ryan HE, Khadivi B, McNulty W, Rickert RC, and Johnson RS. Hypoxia-inducible factor 1alpha is essential for cell cycle arrest during hypoxia. *Molecular and cellular biology*. 2003;23(1):359-69.
109. Shweiki D, Itin A, Soffer D, and Keshet E. Vascular endothelial growth factor induced by hypoxia may mediate hypoxia-initiated angiogenesis. *Nature*. 1992;359(6398):843-5.
110. Shweiki D, Neeman M, Itin A, and Keshet E. Induction of vascular endothelial growth factor expression by hypoxia and by glucose deficiency in multicell spheroids: implications for tumor angiogenesis. *Proceedings of the National Academy of Sciences of the United States of America*. 1995;92(3):768-72.

111. Perkett EA, Badesch DB, Roessler MK, Stenmark KR, and Meyrick B. Insulin-like growth factor I and pulmonary hypertension induced by continuous air embolization in sheep. *American journal of respiratory cell and molecular biology*. 1992;6(1):82-7.
112. Assender JW, Southgate KM, Hallett MB, and Newby AC. Inhibition of proliferation, but not of Ca²⁺ mobilization, by cyclic AMP and GMP in rabbit aortic smooth-muscle cells. *The Biochemical journal*. 1992;288 (Pt 2)(527-32.
113. Benitz WE, Kelley RT, Anderson CM, Lorant DE, and Bernfield M. Endothelial heparan sulfate proteoglycan. I. Inhibitory effects on smooth muscle cell proliferation. *American journal of respiratory cell and molecular biology*. 1990;2(1):13-24.
114. Humphries DE, Lee SL, Fanburg BL, and Silbert JE. Effects of hypoxia and hyperoxia on proteoglycan production by bovine pulmonary artery endothelial cells. *Journal of cellular physiology*. 1986;126(2):249-53.
115. Kesavapany S, Zheng YL, Amin N, and Pant HC. Peptides derived from Cdk5 activator p35, specifically inhibit deregulated activity of Cdk5. *Biotechnology journal*. 2007;2(8):978-87.
116. Bosutti A, Qi J, Pennucci R, Bolton D, Matou S, Ali K, Tsai LH, Krupinski J, Petcu EB, Montaner J, et al. Targeting p35/Cdk5 signalling via CIP-peptide promotes angiogenesis in hypoxia. *PloS one*. 2013;8(9):e75538.
117. Santoro A, Rimassa L, Borbath I, Daniele B, Salvagni S, Van Laethem JL, Van Vlierberghe H, Trojan J, Kolligs FT, Weiss A, et al. Tivantinib for second-line treatment of advanced hepatocellular carcinoma: a randomised, placebo-controlled phase 2 study. *The Lancet Oncology*. 2013;14(1):55-63.
118. Liu Y, Zhang JB, Qin Y, Wang W, Wei L, Teng Y, Guo L, Zhang B, Lin Z, Liu J, et al. PROX1 promotes hepatocellular carcinoma metastasis by way of up-regulating hypoxia-inducible factor 1alpha expression and protein stability. *Hepatology*. 2013;58(2):692-705.
119. Semenza GL. Hypoxia-inducible factors in physiology and medicine. *Cell*. 2012;148(3):399-408.

APPENDIX

7. APPENDIX

7.1 Supplementary data

7.1.1 Mass spectra

Mass spectrometry analysis of CDK5 phosphorylation sites on HIF-1 α was performed by Dr. T. Fröhlich from the Laboratory for Functional Genome Analysis (LAFUGA), Gene Center, University of Munich. MS/MS spectrums and fragmentation tables of *in vitro* and *in vivo* analyses of HIF-1 α are shown below.

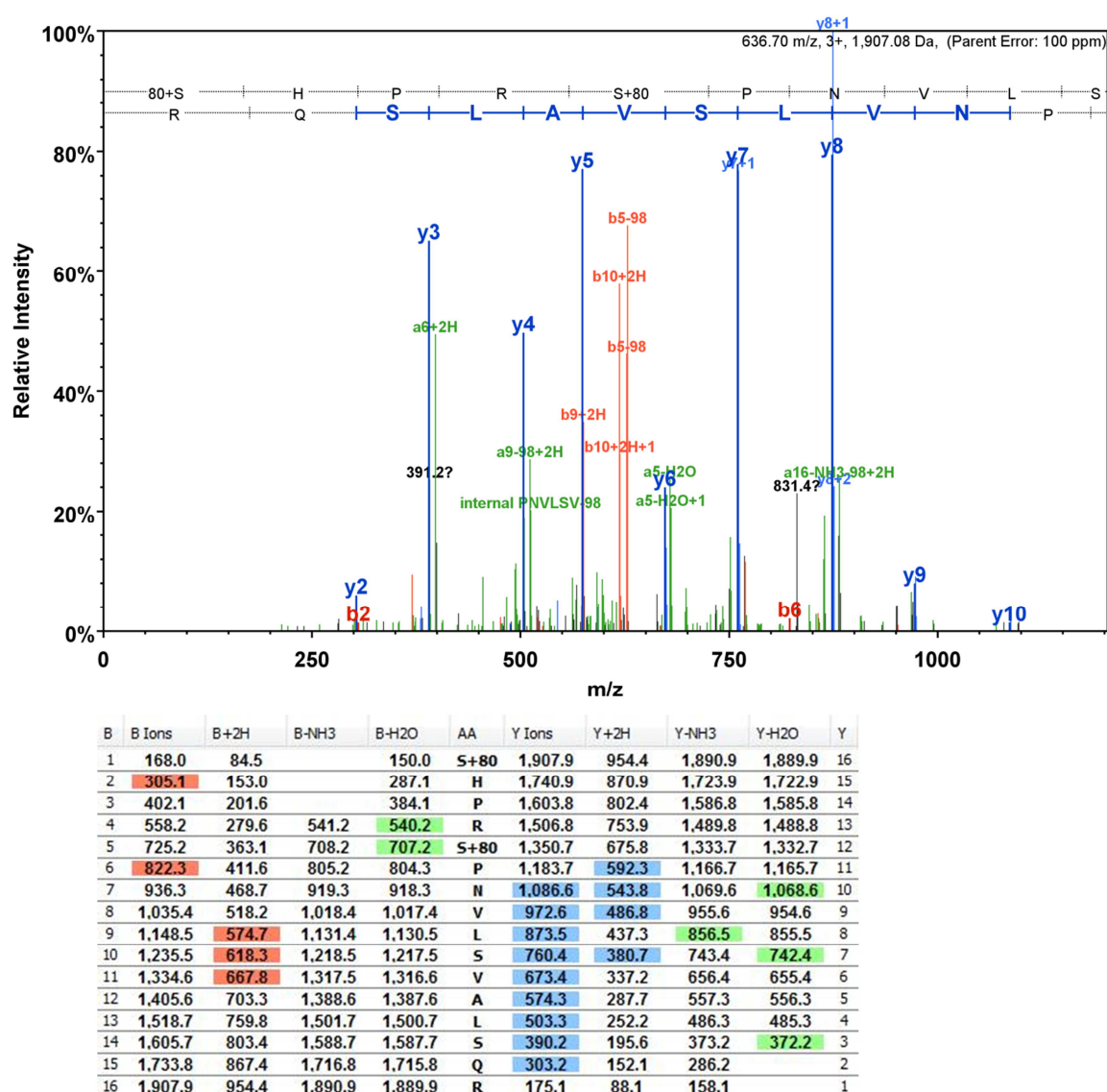


Figure 25: MS/MS spectrum and fragmentation table of peptide $^{683}\text{SHPRSPNVLSVALSQR}^{698}$ of HIF-1 α .

The phosphorylated serines within the peptide sequence are underlined and marked as bold. Detected b ions are highlighted in red and y ions are highlighted in blue. Further signals which could be assigned to other fragment types are highlighted in green.

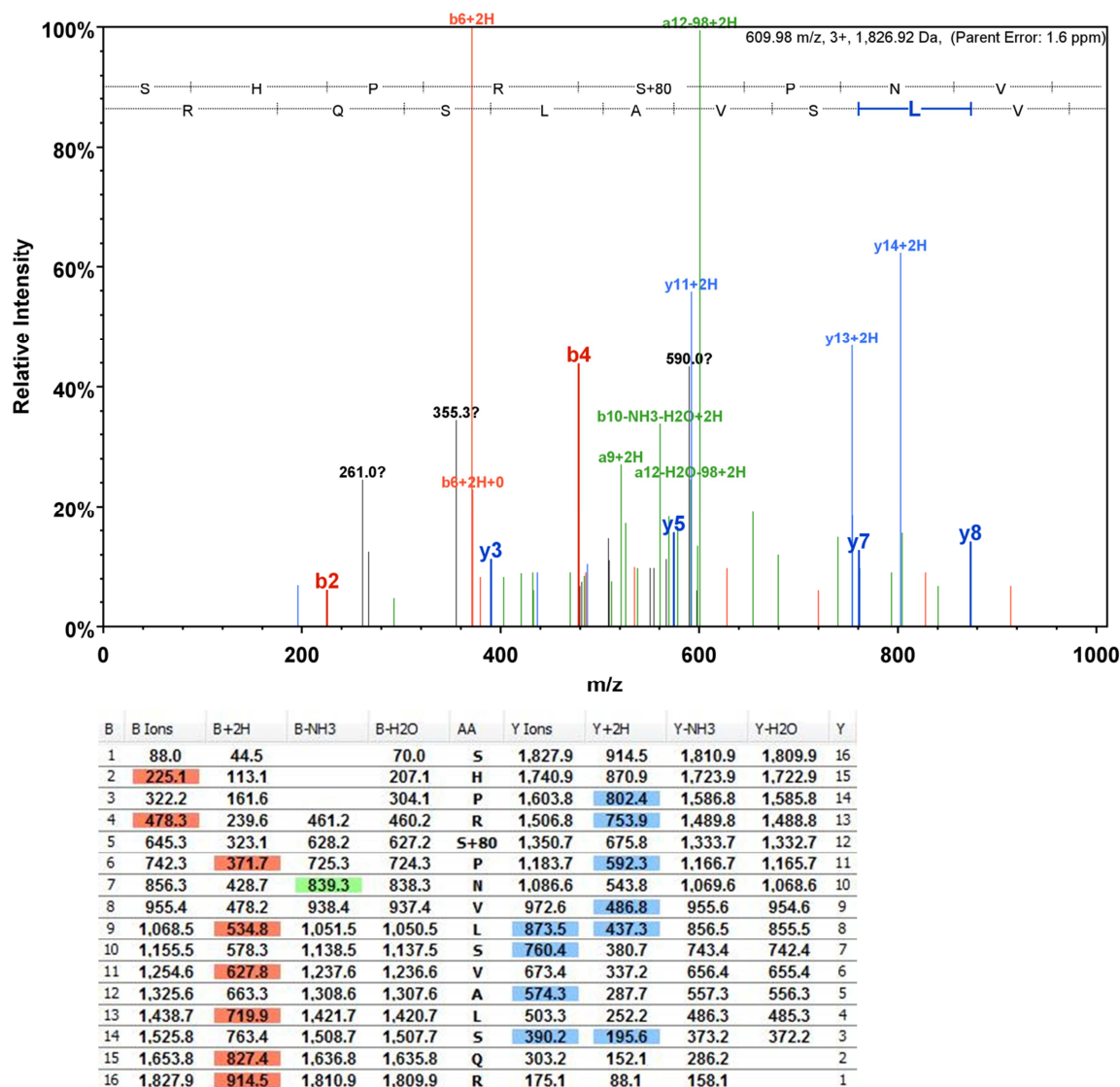


Figure 26: MS/MS spectrum and fragmentation table of peptide

⁶⁸³SHPRSPNVLSVALSQR⁶⁹⁸ of HIF-1 α .

The phosphorylated serine within the peptide sequence is underlined and marked as bold. Detected b ions are highlighted in red and y ions are highlighted in blue. Further signals which could be assigned to other types of fragments are highlighted in green.

7.1.2 Sequence analyses of S687A and S687E mutants

S687A:

CLUSTAL 2.1 multiple sequence alignment

```

WT          TCCGCCCCATTGACGCAAATGGGCGGTAGGCGTGACGGTGGGAGGTCTATATAAGCAGA 60
XL1A1      -----AAGCAGA 7
                      * * * * *

WT          GCTCTCTGGCTAACTAGAGAACCCACTGCTTACTGGCTTATCGAAATTAATACGACTCAC 120
XL1A1      GCTCTCTGGCTAACTAGAGAACCCACTGCTTACTGGCTTATCGAAATTAATACGACTCAC 67
          * * * * *

WT          TATAGGGAGACCCAAGCTTACCATGGCCTACCCNTACGACGTGCCCCGACTACGCCTCCCT 180
XL1A1      TATAGGGAGACCCAAGCTTACCATGGCCTACCCCTACGACGTGCCCCGACTACGCCTCCCT 127
          * * * * *

WT          CGGATCCGCCACCATGGAGGGCGCCGGCGGCGGAACGACAAGAAAAAGATAAGTTCTGA 240
XL1A1      CGGATCCGCCACCATGGAGGGCGCCGGCGGCGGAACGACAAGAAAAAGATAAGTTCTGA 187
          * * * * *

WT          ACGTCGAAAAGAAAAGTCTCGAGATGCAGCCAGATCTCGGCGAAGTAAAGAATCTGAAGT 300
XL1A1      ACGTCGAAAAGAAAAGTCTCGAGATGCAGCCAGATCTCGGCGAAGTAAAGAATCTGAAGT 247
          * * * * *

WT          TTTTATGAGCTTGCTCATCAGTTGCCACTTCCACATAATGTGAGTTTCGCATCTTGATAA 360
XL1A1      TTTTATGAGCTTGCTCATCAGTTGCCACTTCCACATAATGTGAGTTTCGCATCTTGATAA 307
          * * * * *

WT          GGCCTCTGTGATGAGGCTTACCATCAGCTATTTGCGTGTGAGGAACTTCTGGATGCTGG 420
XL1A1      GGCCTCTGTGATGAGGCTTACCATCAGCTATTTGCGTGTGAGGAACTTCTGGATGCTGG 367
          * * * * *

WT          TGATTTGGATATTGAAGATGACATGAAAGCACAGATGAATTGCTTTTATTTGAAAGCCTT 480
XL1A1      TGATTTGGATATTGAAGATGACATGAAAGCACAGATGAATTGCTTTTATTTGAAAGCCTT 427
          * * * * *

WT          GGATGGTTTTGTTATGGTTCTCACAGATGATGGTGACATGATTACATTTCTGATAATGT 540
XL1A1      GGATGGTTTTGTTATGGTTCTCACAGATGATGGTGACATGATTACATTTCTGATAATGT 487
          * * * * *

WT          GAACAAATACATGGGATTAACCTCAGTTTGAACCTAAGTGGACACAGTGTGTTTGATTTTAC 600
XL1A1      GAACAAATACATGGGATTAACCTCAGTTTGAACCTAAGTGGACACAGTGTGTTTGATTTTAC 547
          * * * * *

WT          TCATCCATGTGACCATGAGGAAATGAGAGAAATGCTTACACACAGAAATGGCCTTGTGAA 660
XL1A1      TCATCCATGTGACCATGAGGAAATGAGAGAAATGCTTACACACAGAAATGGCCTTGTGAA 607
          * * * * *

WT          AAAGGGTAAAGAACAAAACACACAGCGAAGCTTTTTTCTCAGAATGAAGTGTAACCTAAC 720
XL1A1      AAAGGGTAAAGAACAAAACACACAGCGAAGCTTTTTTCTCAGAATGAAGTGTAACCTAAC 667
          * * * * *

WT          TAGCCGAGGAAGAACTATGAACATAAAGTCTGCAACATGGAAGGTATTGCACTGCACAGG 780
XL1A1      TAGCCGAGGAAGAACTATGAACATAAAGTCTGCAACATGGAAGGTATTGCACTGCACAGG 727
          * * * * *

WT          CCACATTCACGTATATGATACCAACAGTAACCAACCTCAGTGTGGGTATAAGAAACCACC 840
XL1A1      CCACATTCACGTATATGATACCAACAGTAACCAACCTCAGTGTGGGTATAAGAAACCACC 787
          * * * * *

WT          TATGACCTGCTTGGTGCTGATTTGTGAACCCATTCTCACCATCAAATATTGAAATTCC 900
XL1A1      TATGACCTGCTTGGTGCTGATTTGTGAACCCATTCTCACCATCAAATATTGAAATTCC 847
          * * * * *

```

WT	TTTAGATAGCAAGACTTTCCTCAGTCGACACAGCCTGGATATGAAATTTTCTTATTGTGA	960
XL1A1	TTTAGATAGCAAGACTTTCCTCAGTCGACACAGCCTGGATATGAAATTTTCTTATTGTGA	907

WT	TGAAAGAATTACCGAATTGATGGGATATGAGCCAGAAGAAGCTTTTAGGCCGCTCAATTTA	1020
XL1A1	TGAAAGAATTACCGAATTGATGGGATATGAGCCAGAAGAAGCTTTTAGGCCGCTCAATTTA	967

WT	TGAATATTATCATGCTTTGGACTCTGATCATCTGACCAAACTCATCATGATATGTTTAC	1080
XL1A1	TGAATATTATCATGCTTTGGACTCTGATCATCTGACCAAACTCATCATGATATGTTTAC	1027

WT	TAAAGGACAAGTCACCACAGGACAGTACAGGATGCTTGCCAAAAGAGGTGGATATGTCTG	1140
XL1A1	TAAAGGACAAGTCACCACAGGACAGTACAGGATGCTTGCCAAAAGAGGTGGATATGTCTG	1087

WT	GGTTGAAACTCAAGCAACTGTTCATATATAACACCAAGAATTCTCAACCACAGTGCATTGT	1200
XL1A1	GGTTGAAACTCAAGCAACTGTTCATATATAACACCAAGAATTCTCAACCACAGTGCATTGT	1147

WT	ATGTGTGAATTACGTTGTGAGTGGTATTATTTCAGCAGCACTTGATTTTCTCCCTTCAACA	1260
XL1A1	ATGTGTGAATTACGTTGTGAGTGGTATTATTTCAGCAGCACTTGATTTTCTCCCTTCAACA	1207

WT	AACAGAATGTGTCCTTAAACCGGTTGAATCTTCAGATATGAAAATGACTCAGCTATTCAC	1320
XL1A1	AACAGAATGTGTCCTTAAACCGGTTGAATCTTCAGATATGAAAATGACTCAGCTATTCAC	1267

WT	CAAAGTTGAATCAGAAGATACAAGTAGCCTCTTTGACAAACTTAAGAAGGAACCTGATGC	1380
XL1A1	CAAAGTTGAATCAGAAGATACAAGTAGCCTCTTTGACAAACTTAAGAAGGAACCTGATGC	1327

WT	TTTAACTTTGCTGGCCCCAGCCGCTGGAGACACAATCATATCTTTAGATTTTGGCAGCAA	1440
XL1A1	TTTAACTTTGCTGGCCCCAGCCGCTGGAGACACAATCATATCTTTAGATTTTGGCAGCAA	1387

WT	CGACACAGAACTGATGACCAGCAACTTGAGGAAGTACCATTATATAATGATGTAATGCT	1500
XL1A1	CGACACAGAACTGATGACCAGCAACTTGAGGAAGTACCATTATATAATGATGTAATGCT	1447

WT	CCCCTCACCCAACGAAAAATTACAGAATATAAATTTGGCAATGTCTCCATTACCCACCGC	1560
XL1A1	CCCCTCACCCAACGAAAAATTACAGAATATAAATTTGGCAATGTCTCCATTACCCACCGC	1507

WT	TGAAACGCCAAAGCCACTTCGAAGTAGTGCTGACCCTGCACTCAATCAAGAAGTTGCATT	1620
XL1A1	TGAAACGCCAAAGCCACTTCGAAGTAGTGCTGACCCTGCACTCAATCAAGAAGTTGCATT	1567

WT	AAAATTAGAACCAATCCAGAGTCACTGGAACCTTCTTTTACCATGCCCCAGATTCAGGA	1680
XL1A1	AAAATTAGAACCAATCCAGAGTCACTGGAACCTTCTTTTACCATGCCCCAGATTCAGGA	1627

WT	TCAGACACCTAGTCCTTCCGATGGAAGCACTAGACAAAGTTCACCTGAGCCTAATAGTCC	1740
XL1A1	TCAGACACCTAGTCCTTCCGATGGAAGCACTAGACAAAGTTCACCTGAGCCTAATAGTCC	1687

WT	CAGTGAATATTGTTTTTATGTGGATAGTGATATGGTCAATGAATTCAAGTTGGAATTGGT	1800
XL1A1	CAGTGAATATTGTTTTTATGTGGATAGTGATATGGTCAATGAATTCAAGTTGGAATTGGT	1747

WT	AGAAAACTTTTGTGTAAGACACAGAAGCAAAGAACCCATTTTCTACTCAGGACACAGA	1860
XL1A1	AGAAAACTTTTGTGTAAGACACAGAAGCAAAGAACCCATTTTCTACTCAGGACACAGA	1807

WT	TTTAGACTTGGAGATGTTAGCTCCCTATATCCCAATGGATGATGACTTCCAGTTACGTTT	1920
XL1A1	TTTAGACTTGGAGATGTTAGCTCCCTATATCCCAATGGATGATGACTTCCAGTTACGTTT	1867

WT	CTTCGATCAGTTGTCACCATTAGAAAGCAGTTCCGCAAGCCCTGAAAGCGCAAGTCTCTCA	1980
XL1A1	CTTCGATCAGTTGTCACCATTAGAAAGCAGTTCCGCAAGCCCTGAAAGCGCAAGTCTCTCA	1927

WT	AAGCACAGTTACAGTATTCCAGCAGACTCAAATACAAGAACCTACTGCTAATGCCACCAC	2040
XL1A1	AAGCACAGTTACAGTATTCCAGCAGACTCAAATACAAGAACCTACTGCTAATGCCACCAC	1987

WT	TACCACTGCCACCACTGATGAATTA AAAACAGTGACAAAAGACCGTATGGAAGACATTAA	2100
XL1A1	TACCACTGCCACCACTGATGAATTA AAAACAGTGACAAAAGACCGTATGGAAGACATTAA	2047

WT	AATATTGATTGCATCTCCATCTCCTACCCACATACATAAAGAACTACTAGTGCCACATC	2160
XL1A1	AATATTGATTGCATCTCCATCTCCTACCCACATACATAAAGAACTACTAGTGCCACATC	2107

WT	ATCACCATATAGAGATACTCAAAGTCGGACAGCCTCACCAAACAGAGCAGGAAAAGGAGT	2220
XL1A1	ATCACCATATAGAGATACTCAAAGTCGGACAGCCTCACCAAACAGAGCAGGAAAAGGAGT	2167

WT	CATAGAACAGACAGAAAAATCTCATCCAAGAGCCTAACGTGTTATCTGTCGCTTTGAG	2280
XL1A1	CATAGAACAGACAGAAAAATCTCATCCAAGAGCTAACGTGTTATCTGTCGCTTTGAG	2227

WT	TCAAAGAACTACAGTTCCTGAGGAAGAACTAAATCCAAAGATACTAGCTTTGCAGAATGC	2340
XL1A1	TCAAAGAACTACAGTTCCTGAGGAAGAACTAAATCCAAAGATACTAGCTTTGCAGAATGC	2287

WT	TCAGAGAAAGCGAAAAATGGAACATGATGGTTCACTTTTTCAAGCAGTAGGAATTGGAAC	2400
XL1A1	TCAGAGAAAGCGAAAAATGGAACATGATGGTTCACTTTTTCAAGCAGTAGGAATTGGAAC	2347

WT	ATTATTACAGCAGCCAGACGATCATGCAGCTACTACATCACTTTCTTGGAACCGTGTA	2460
XL1A1	ATTATTACAGCAGCCAGACGATCATGCAGCTACTACATCACTTTCTTGGAACCGTGTA	2407

WT	AGGATGCAAATCTAGTGAACAGAATGGAATGGAGCAAAAGACAATTATTTTAATACCCTC	2520
XL1A1	AGGATGCAAATCTAGTGAACAGAATGGAATGGAGCAAAAGACAATTATTTTAATACCCTC	2467

WT	TGATTTAGCATGTAGACTGCTGGGGCAATCAATGGATGAAAGTGGATTACCACAGCTGAC	2580
XL1A1	TGATTTAGCATGTAGACTGCTGGGGCAATCAATGGATGAAAGTGGATTACCACAGCTGAC	2527

WT	CAGTTATGATTGTGAAGTTAATGCTCCTATACAAGGCAGCAGAAACCTACTGCAGGGTGA	2640
XL1A1	CAGTTATGATTGTGAAGTTAATGCTCCTATACAAGGCAGCAGAAACCTACTGCAGGGTGA	2587

WT	AGAATTACTCAGAGCTTTGGATCAAGTTAACTGACAATTCTGCAGATATCCATCACACTG	2700
XL1A1	AGAATTACTCAGAGCTTTGGATCAAGTTAACTGACAATTCTGCAGATATCCATCACACTG	2647

WT	GCGGCCGCTCGAGCATGCATCTAGAGG	2727
XL1A1	GCGGCC-----	2653

S687E:

CLUSTAL 2.1 multiple sequence alignment

```

WT          TCCGCCCCATTGACGCAAATGGGCGGTAGGCGGTGTACGGTGGGAGGTCTATATAAGCAGA 60
XL1E11      -----CAGA 4
                                     ****

WT          GCTCTCTGGCTAACTAGAGAACCCACTGCTTACTGGCTTATCGAAATTAATACGACTCAC 120
XL1E11      GCTCTCTGGCTAACTAGAGAACCCACTGCTTACTGGCTTATCGAAATTAATACGACTCAC 64
*****

WT          TATAGGGAGACCCAAGCTTACCATGGCCTACCCNTACGACGTGCCCGACTACGCCTCCCT 180
XL1E11      TATAGGGAGACCCAAGCTTACCATGGCCTACCCCTACGACGTGCCCGACTACGCCTCCCT 124
*****

WT          CGGATCCGCCACCATGGAGGGCGCCGGCGGCGCGAACGACAAGAAAAAGATAAGTTCTGA 240
XL1E11      CGGATCCGCCACCATGGAGGGCGCCGGCGGCGCGAACGACAAGAAAAAGATAAGTTCTGA 184
*****

WT          ACGTCGAAAAGAAAAGTCTCGAGATGCAGCCAGATCTCGGCGAAGTAAAGAATCTGAAGT 300
XL1E11      ACGTCGAAAAGAAAAGTCTCGAGATGCAGCCAGATCTCGGCGAAGTAAAGAATCTGAAGT 244
*****

WT          TTTTATGAGCTTGCTCATCAGTTGCCACTTCCACATAATGTGAGTTTCGCATCTTGATAA 360
XL1E11      TTTTATGAGCTTGCTCATCAGTTGCCACTTCCACATAATGTGAGTTTCGCATCTTGATAA 304
*****

WT          GGCCTCTGTGATGAGGCTTACCATCAGCTATTTGCGTGTGAGGAACTTCTGGATGCTGG 420
XL1E11      GGCCTCTGTGATGAGGCTTACCATCAGCTATTTGCGTGTGAGGAACTTCTGGATGCTGG 364
*****

WT          TGATTTGGATATTGAAGATGACATGAAAGCACAGATGAATTGCTTTTATTTGAAAGCCTT 480
XL1E11      TGATTTGGATATTGAAGATGACATGAAAGCACAGATGAATTGCTTTTATTTGAAAGCCTT 424
*****

WT          GGATGGTTTTGTTATGGTTCTCACAGATGATGGTGACATGATTTACATTTCTGATAATGT 540
XL1E11      GGATGGTTTTGTTATGGTTCTCACAGATGATGGTGACATGATTTACATTTCTGATAATGT 484
*****

WT          GAACAAATACATGGGATTAACCTCAGTTTGAACCTAACTGGACACAGTGTGTTTGATTTTAC 600
XL1E11      GAACAAATACATGGGATTAACCTCAGTTTGAACCTAACTGGACACAGTGTGTTTGATTTTAC 544
*****

WT          TCATCCATGTGACCATGAGGAAATGAGAGAAATGCTTACACACAGAAATGGCCTTGTGAA 660
XL1E11      TCATCCATGTGACCATGAGGAAATGAGAGAAATGCTTACACACAGAAATGGCCTTGTGAA 604
*****

WT          AAAGGGTAAAGAACAAAACACACAGCGAAGCTTTTTTCTCAGAATGAAGTGTAACCTAAC 720
XL1E11      AAAGGGTAAAGAACAAAACACACAGCGAAGCTTTTTTCTCAGAATGAAGTGTAACCTAAC 664
*****

WT          TAGCCGAGGAAGAACTATGAACATAAAGTCTGCAACATGGAAGGTATTGCACTGCACAGG 780
XL1E11      TAGCCGAGGAAGAACTATGAACATAAAGTCTGCAACATGGAAGGTATTGCACTGCACAGG 724
*****

WT          CCACATTACGTATATGATACCAACAGTAACCAACCTCAGTGTGGGTATAAGAAACCACC 840
XL1E11      CCACATTACGTATATGATACCAACAGTAACCAACCTCAGTGTGGGTATAAGAAACCACC 784
*****

WT          TATGACCTGCTTGGTGCTGATTGTGAACCCATTCTCACCATCAAATATTGAAATTCC 900
XL1E11      TATGACCTGCTTGGTGCTGATTGTGAACCCATTCTCACCATCAAATATTGAAATTCC 844
*****

```

WT	TTTAGATAGCAAGACTTTCCTCAGTCGACACAGCCTGGATATGAAATTTTCTTATTGTGA	960
XL1E11	TTTAGATAGCAAGACTTTCCTCAGTCGACACAGCCTGGATATGAAATTTTCTTATTGTGA	904

WT	TGAAAGAATTACCGAATTGATGGGATATGAGCCAGAAGAAGCTTTTAGGCCGCTCAATTTA	1020
XL1E11	TGAAAGAATTACCGAATTGATGGGATATGAGCCAGAAGAAGCTTTTAGGCCGCTCAATTTA	964

WT	TGAATATTATCATGCTTTGGACTCTGATCATCTGACCAAACTCATCATGATATGTTTAC	1080
XL1E11	TGAATATTATCATGCTTTGGACTCTGATCATCTGACCAAACTCATCATGATATGTTTAC	1024

WT	TAAAGGACAAGTCACCACAGGACAGTACAGGATGCTTGCCAAAAGAGGTGGATATGTCTG	1140
XL1E11	TAAAGGACAAGTCACCACAGGACAGTACAGGATGCTTGCCAAAAGAGGTGGATATGTCTG	1084

WT	GGTTGAAACTCAAGCAACTGTTCATATATAACACCAAGAATTCTCAACCACAGTGCATTGT	1200
XL1E11	GGTTGAAACTCAAGCAACTGTTCATATATAACACCAAGAATTCTCAACCACAGTGCATTGT	1144

WT	ATGTGTGAATTACGTTGTGAGTGGTATTATTACGACGACTTGATTTTCTCCCTTCAACA	1260
XL1E11	ATGTGTGAATTACGTTGTGAGTGGTATTATTACGACGACTTGATTTTCTCCCTTCAACA	1204

WT	AACAGAATGTGTCCTTAAACCGGTTGAATCTTCAGATATGAAAATGACTCAGCTATTCAC	1320
XL1E11	AACAGAATGTGTCCTTAAACCGGTTGAATCTTCAGATATGAAAATGACTCAGCTATTCAC	1264

WT	CAAAGTTGAATCAGAAGATACAAGTAGCCTCTTTGACAAACTTAAGAAGGAACCTGATGC	1380
XL1E11	CAAAGTTGAATCAGAAGATACAAGTAGCCTCTTTGACAAACTTAAGAAGGAACCTGATGC	1324

WT	TTTAACTTTGCTGGCCCCAGCCGCTGGAGACACAATCATATCTTTAGATTTTGGCAGCAA	1440
XL1E11	TTTAACTTTGCTGGCCCCAGCCGCTGGAGACACAATCATATCTTTAGATTTTGGCAGCAA	1384

WT	CGACACAGAACTGATGACCAGCAACTTGAGGAAGTACCATTATATAATGATGTAATGCT	1500
XL1E11	CGACACAGAACTGATGACCAGCAACTTGAGGAAGTACCATTATATAATGATGTAATGCT	1444

WT	CCCCTCACCCAACGAAAAATTACAGAATATAAATTTGGCAATGTCTCCATTACCCACCGC	1560
XL1E11	CCCCTCACCCAACGAAAAATTACAGAATATAAATTTGGCAATGTCTCCATTACCCACCGC	1504

WT	TGAAACGCCAAAGCCACTTCGAAGTAGTGCTGACCCTGCACTCAATCAAGAAGTTGCATT	1620
XL1E11	TGAAACGCCAAAGCCACTTCGAAGTAGTGCTGACCCTGCACTCAATCAAGAAGTTGCATT	1564

WT	AAAATTAGAACCAAATCCAGAGTCACTGGAACCTTCTTTTACCATGCCCCAGATTCAGGA	1680
XL1E11	AAAATTAGAACCAAATCCAGAGTCACTGGAACCTTCTTTTACCATGCCCCAGATTCAGGA	1624

WT	TCAGACACCTAGTCCTTCCGATGGAAGCACTAGACAAAGTTCACCTGAGCCTAATAGTCC	1740
XL1E11	TCAGACACCTAGTCCTTCCGATGGAAGCACTAGACAAAGTTCACCTGAGCCTAATAGTCC	1684

WT	CAGTGAATATTGTTTTTATGTGGATAGTGATATGGTCAATGAATTCAAGTTGGAATTGGT	1800
XL1E11	CAGTGAATATTGTTTTTATGTGGATAGTGATATGGTCAATGAATTCAAGTTGGAATTGGT	1744

WT	AGAAAACTTTTGTGTAAGACACAGAAGCAAAGAACCCATTTTCTACTCAGGACACAGA	1860
XL1E11	AGAAAACTTTTGTGTAAGACACAGAAGCAAAGAACCCATTTTCTACTCAGGACACAGA	1804

WT	TTTAGACTTGGAGATGTTAGCTCCCTATATCCCAATGGATGATGACTTCCAGTTACGTTTC	1920
XL1E11	TTTAGACTTGGAGATGTTAGCTCCCTATATCCCAATGGATGATGACTTCCAGTTACGTTTC	1864

WT	CTTCGATCAGTTGTCACCATTAGAAAGCAGTTCCGCAAGCCCTGAAAGCGCAAGTCCCTCA	1980
XL1E11	CTTCGATCAGTTGTCACCATTAGAAAGCAGTTCCGCAAGCCCTGAAAGCGCAAGTCCCTCA	1924

WT	AAGCACAGTTACAGTATTCCAGCAGACTCAAATACAAGAACCTACTGCTAATGCCACCAC	2040
XL1E11	AAGCACAGTTACAGTATTCCAGCAGACTCAAATACAAGAACCTACTGCTAATGCCACCAC	1984

WT	TACCACTGCCACCACTGATGAATTA AAAACAGTGACAAAAGACCGTATGGAAGACATTAA	2100
XL1E11	TACCACTGCCACCACTGATGAATTA AAAACAGTGACAAAAGACCGTATGGAAGACATTAA	2044

WT	AATATTGATTGCATCTCCATCTCCTACCCACATACATAAAGAACTACTAGTGCCACATC	2160
XL1E11	AATATTGATTGCATCTCCATCTCCTACCCACATACATAAAGAACTACTAGTGCCACATC	2104

WT	ATCACCATATAGAGATACTCAAAGTCGGACAGCCTCACCAAACAGAGCAGGAAAAGGAGT	2220
XL1E11	ATCACCATATAGAGATACTCAAAGTCGGACAGCCTCACCAAACAGAGCAGGAAAAGGAGT	2164

WT	CATAGAACAGACAGAAAAATCTCATCCAAGAGCCTAACGTGTTATCTGTCGCTTTGAG	2280
XL1E11	CATAGAACAGACAGAAAAATCTCATCCAAGAGCCTAACGTGTTATCTGTCGCTTTGAG	2224

WT	TCAAAGAACTACAGTTCCTGAGGAAGAACTAAATCCAAAGATACTAGCTTTGCAGAATGC	2340
XL1E11	TCAAAGAACTACAGTTCCTGAGGAAGAACTAAATCCAAAGATACTAGCTTTGCAGAATGC	2284

WT	TCAGAGAAAGCGAAAAATGGAACATGATGGTTCACTTTTTCAAGCAGTAGGAATTGGAAC	2400
XL1E11	TCAGAGAAAGCGAAAAATGGAACATGATGGTTCACTTTTTCAAGCAGTAGGAATTGGAAC	2344

WT	ATTATTACAGCAGCCAGACGATCATGCAGCTACTACATCACTTTCTTGAAACGTGTAAA	2460
XL1E11	ATTATTACAGCAGCCAGACGATCATGCAGCTACTACATCACTTTCTTGAAACGTGTAAA	2404

WT	AGGATGCAAATCTAGTGAACAGAATGGAATGGAGCAAAAGACAATTATTTTAATACCCTC	2520
XL1E11	AGGATGCAAATCTAGTGAACAGAATGGAATGGAGCAAAAGACAATTATTTTAATACCCTC	2464

WT	TGATTTAGCATGTAGACTGCTGGGGCAATCAATGGATGAAAGTGGATTACCACAGCTGAC	2580
XL1E11	TGATTTAGCATGTAGACTGCTGGGGCAATCAATGGATGAAAGTGGATTACCACAGCTGAC	2524

WT	CAGTTATGATTGTGAAGTTAATGCTCCTATACAAGGCAGCAGAAACCTACTGCAGGGTGA	2640
XL1E11	CAGTTATGATTGTGAAGTTAATGCTCCTATACAAGGCAGCAGAAACCTACTGCAGGGTGA	2584

WT	AGAATTACTCAGAGCTTTGGATCAAGTTAACTGACAATTCTGCAGATATCCATCACACTG	2700
XL1E11	AGAATTACTCAGAGCTTTGGATCAAGTTAACTGACAATTCTGCAGATATCCATCACACTG	2644

WT	GCGGCCGCT-CGAGCATGCATCTAGAGG	2727
XL1E11	GCGGCCGCTTCGA-----	2657

Figure 27: Point mutations at serine 687 to either alanine or glutamate were introduced in HIF-1 α by site-directed mutagenesis.

Sequence alignment of wildtype HIF-1 α (wt) with the alanine (clone XL1A1) and glutamate (clone XL1E11) mutant of serine 687 is shown. Mutated sites are indicated in red.

7.2 Abbreviations

AEC	3-amino-9-ethylcarbazole
ANOVA	analysis of variance
ATM	ataxia telangiectasia mutated
ATP	adenosine 5' tri-phosphat
BA12	(2-[[[2-[(4-aminocyclohexyl)amino]-9-cyclopentyl-purin-6-yl]amino]methyl]-4-chloro-phenol)
bHLH	basic-helix-loop-helix
BP14	(N2-(4-aminocyclohexyl)-9-cyclopentyl-N6-[[6-(2-furyl)-3-pyridyl]methyl]purine-2,6-diamine)
BSA	bovine serum albumin
c-Abl	c-Abelson
CBP	CREB-binding protein
CD31	cluster of differentiation 31
CDK	cyclin-dependent kinase
CREB	cAMP response element-binding protein
C-TAD	C-terminal transactivation domain
DEN	diethylnitrosamine
DFO	deferoxamine
DMEM	Dulbecco's Modified Eagle Medium
DMSO	dimethyl sulfoxide
DNA	deoxyribonucleic acid
DTT	dithiothreitol
ECGM	endothelial cell growth medium
EDTA	ethylene diamine tetraacetic acid
EGTA	ethylene glycol tetraacetic acid
EMT	epithelial-mesenchymal transition
EPC	endothelial progenitor cells
FCS	fetal calf serum
FIH-1	factor-inhibiting-HIF-1
HA	hemagglutinin
HCC	hepatocellular carcinoma
HEPES	4-(2-hydroxyethyl)-1-piperazineethanesulfonic acid
HIF	hypoxia-inducible factor
HRP	horseradish peroxidase
HUVEC	human umbilical vein endothelial cells

JCRB	Japanese Collection of Research Bioresources
MET	mesenchymal-epithelial transition
MMP	matrix metalloproteinase
mTOR	mammalian target of rapamycin
NES	nuclear export signal
NLS	nuclear localization signal
nt	non-targeting
N-TAD	N-terminal transactivation domain
ODDD	oxygen-dependent degradation domain
PAS	PER-ARNT-SIM
PDGF	platelet-derived growth factor
PDH	prolyl hydroxylase
PF	pro-angiogenic factors
PLGF	placental growth factor
PMSF	phenylmethylsulfonyl fluoride
PROX1	prospero homeobox 1
Rac1	Ras-related C3 botulinum toxin substrate 1
RT	room temperature
SCID	severe combined immunodeficiency
SDS	Sodium dodecyl sulfate
SEM	standard error of mean
shRNA	short hairpin RNA
siRNA	small interfering RNA
T/E	trypsin/EDTA
VEGF	vascular endothelial growth factor
VEGFR1	vascular endothelial growth factor receptor 1
VHL	Von Hippel-Lindau protein
wt	wild-type

7.3 Publications

7.3.1 Original publication

Cyclin-dependent kinase 5 regulates HIF-1 α stability in hepatocellular carcinoma

Julia Herzog¹, Sandra M. Ehrlich¹, Johanna Liebl¹, Thomas Fröhlich², Georg J. Arnold², Wolfgang Mikulits³, Angelika M. Vollmar¹, Stefan Zahler¹

¹Department Pharmacy, Pharmaceutical Biology, University of Munich, Butenandtstr. 5-13, 81377 Munich, Germany

²Laboratory for Functional Genome Analysis (LAFUGA), Gene Center Munich, University of Munich, Feodor-Lynen-Straße 25, 81377 Munich, Germany

³Department of Medicine I, Division: Institute of Cancer Research, Comprehensive Cancer Center Vienna, Medical University of Vienna, Borschke-Gasse 8A, 1090 Vienna, Austria

In preparation

7.3.2 Poster presentations

CDK5 stabilizes HIF-1 α in endothelial and liver tumor cells: a novel signaling mechanism important for HCC therapy

Julia Herzog¹, Sandra M. Stamm¹, Johanna Liebl¹, Angelika M. Vollmar¹, Stefan Zahler¹

¹Department of Pharmacy, Pharmaceutical Biology, University of Munich, Munich, Germany

SPSAS – Advances in Molecular Oncology: Translating Molecular Biology into Cancer Treatment 2013, February 3-8, São Paulo, Brazil.

CDK5 regulates angiogenesis via stabilizing HIF-1 α in endothelial and liver tumor cells: a novel signaling mechanism with potential importance for HCC therapy

Herzog, J.¹; Ehrlich, S. M.¹; Liebl, J.¹; Fröhlich, T.²; Mikulits, W.³; Vollmar, A.M.¹; Zahler, S.¹

¹Department of Pharmacy, Pharmaceutical Biology, University of Munich, Butenandtstr. 5-13, 81377 Munich, Germany

²Gene Center Munich, University of Munich, Feodor-Lynen-Strasse 25, 81377 Munich, Germany

³Department of Medicine I, Division: Institute of Cancer Research, Comprehensive Cancer Center Vienna, Medical University of Vienna, Spitalgasse 23, 1090 Vienna, Austria

Deutsche Pharmazeutische Gesellschaft (DPhG) Tagung 2014, September 24-26th, Frankfurt, Germany.

7.4 Danksagung

An allererster Stelle möchte ich mich herzlich bei Frau Prof. Vollmar und Herrn Prof. Zahler bedanken, dafür, dass Sie mir ermöglicht haben, bei Ihnen zu promovieren. Die letzten drei Jahre haben mich wissenschaftlich und auch persönlich sehr weitergebracht. Danke für die vielen wertvollen Tipps, Ideen und Ratschläge. Herr Zahler, ich danke Ihnen, dass Sie immer eine offene Tür hatten und ich jederzeit mit meinen Ideen zu Ihnen kommen konnte. Danke für Ihr Vertrauen in meine Arbeit und für die vielen konstruktiven Gespräche.

Ein weiterer Dank geht an Herrn Prof. Wahl-Schott, Herrn Prof. Wagner, Herrn PD Michalakakis sowie Herrn Prof. Frieß. Danke, dass Sie sich die Zeit genommen haben, Teil meines Prüfungskomitees zu sein.

Außerdem möchte ich mich bei unseren Kooperationspartnern bedanken: Herrn Dr. Thomas Fröhlich vom Genzentrum der LMU München für die neuen Einblicke in die Massenspektrometrie. Herrn Prof. Mikulits von der medizinischen Universität Wien für die Kooperation bei den Lösungsmittel-induzierten bzw. HepG2 *in vivo* Versuchen.

Ein ganz besonders großes Dankeschön geht natürlich an alle jetzigen und ehemaligen Mitglieder des AK Vollmars für das sehr gute Arbeitsklima und die vielen spaßigen Aktivitäten auch außerhalb des Laboralltages:

Hanna, danke für deine Hilfe bei den HUH7 *in vivo* Versuchen und dass ich auch sonst immer mit Fragen zu dir kommen konnte.

Lena, danke für die schöne und vor allem stets lustige Zeit, die wir zusammen in unserer Box hatten und dafür, dass du mich so herzlich in die Gruppe aufgenommen hast.

Sandra, Henri, Lina und Max, danke für den Spaß den wir im und außerhalb des Labors hatten. Nicht zuletzt wegen euch bin ich immer sehr gerne zur Arbeit gekommen. Ich hoffe, wir werden auch in Zukunft noch in Kontakt bleiben und viele lustige Abende zusammen erleben.

Sandra, dir möchte ich ganz besonders danken. Es war mir eine große Freude mit dir zusammen zu arbeiten und so manche CDK5 Diskussion zu führen – du hattest immer ein offenes Ohr und viele wertvolle Tipps für mich.

Ein riesiges Dankeschön geht an meine Familie. Danke, dass ihr mich immer und in jeder Lebenslage unterstützt und in meiner Arbeit bestärkt habt. Besonders möchte ich mich bei meinen Eltern bedanken, die in jeglicher Hinsicht die Grundsteine für meinen Weg gelegt haben.

Benedict, danke, dass du immer für mich da bist, für deine bedingungslose Unterstützung und dass du mich auch in angespannter und gestresster Laune erträgst. Ich freue mich auf eine gemeinsame Zukunft mit dir.